Automatica 158 (2023) 111238

Contents lists available at ScienceDirect

Automatica

journal homepage: www.elsevier.com/locate/automatica

Surviving disturbances: A predictive control framework with guaranteed safety☆

Yunda Yan [a,*], Xue-Fang Wang [b], Benjamin James Marshall [c], Cunjia Liu [c], Jun Yang [c], Wen-Hua Chen [c]

[a] Department of Computer Science, University College London, London, WC1E 6BT, UK
[b] School of Engineering, University of Leicester, Leicestershire, LE1 7RH, UK
[c] Department of Aeronautical and Automotive Engineering, Loughborough University, Leicestershire, LE11 3TU, UK

ARTICLE INFO

Article history:
Received 29 August 2022
Received in revised form 4 April 2023
Accepted 5 July 2023
Available online xxxx

Keywords:
Model predictive control
Disturbance rejection
Disturbance observer
Offset-free tracking
Aerial physical interaction

ABSTRACT

Rejecting all disturbances is an extravagant hope in safety-critical control systems, hence surviving them where possible is a sensible objective a controller can deliver. In order to build a theoretical framework starting from surviving all disturbances but taking the appropriate opportunity to reject them, a sufficient condition on surviving disturbances is first established by exploring the relation among steady sets of state, input, and disturbance, followed by an output reachability condition on rejecting disturbances. A new robust safety-critical model prediction control (MPC) framework is then developed by embedding the quartet of pseudo steady input, output, state, and disturbance (IOSD) into the optimisation. Unlike most existing tracking MPC setups, a new and unique formulation is adopted by taking the *pseudo steady disturbance* as an optimisation decision variable, rather than directly driven by the disturbance estimate. This new setup is able to decouple estimation error dynamics, significantly contributing to the guarantee of recursive feasibility, even if the disturbance or its estimate changes rapidly. Moreover, towards optimal coexistence with disturbances, offset-free tracking of a compromised reference can be achieved, if rejecting the disturbance conflicts with safety-critical specifications. Finally, the benefits of the proposed method have been demonstrated by both numerical simulations and experiments on aerial physical interaction.

1. Introduction

1.1. Motivation

Embedding safety constraints into the control design would benefit many robotic systems operated in uncertain environments, ranging from manipulators to mobile platforms (Ferraguti et al., 2022). However, it is recognised that safety-critical control for robotics is susceptible to disturbances, either in the high-level decision-making or in the low-level control performance (Hewing, Wabersich, Menner, & Zeilinger, 2020). An example of aerial physical interaction, as illustrated by Fig. 1, implies that unexpected disturbances may result in catastrophic behaviour. Since it could be risky to continue the original landing decision in the occurrence of the strong wind, staying at such a critical point can be regarded as an acceptable compromise informed by the safety guarantee.

Motivated by this example, it may be too ambitious for the safety-critical systems to reject all the disturbances to reach the predefined specifications. An alternative way is to first guarantee safety under all possible disturbance realisations but take the opportunity to achieve the given objective if the disturbance can be safely rejected. Following this thinking, a unified framework is presented here for the tracking problem of constrained, linear, dynamic systems in the presence of bounded disturbances, which contains not only several sufficient conditions on disturbance survival and rejection but also a new optimisation-based controller with the guarantee of safety[1] and stability.

1.2. Related work

The optimal and safety-critical control design with specific safety guarantee broadly falls into two categories, although it is

☆ The material in this paper was not presented at any conference. This paper was recommended for publication in revised form by Associate Editor Prashant Mhaskar under the direction of Editor Thomas Parisini.

* Corresponding author.
E-mail addresses: yunda.yan@ucl.ac.uk (Y. Yan), xw259@leicester.ac.uk (X.-F. Wang), b.marshall@lboro.ac.uk (B.J. Marshall), c.liu5@lboro.ac.uk (C. Liu), j.yang3@lboro.ac.uk (J. Yang), w.chen@lboro.ac.uk (W.-H. Chen).

[1] The safety here is concerned with the satisfaction of all constraints throughout the entire duration of system operation.

https://doi.org/10.1016/j.automatica.2023.111238

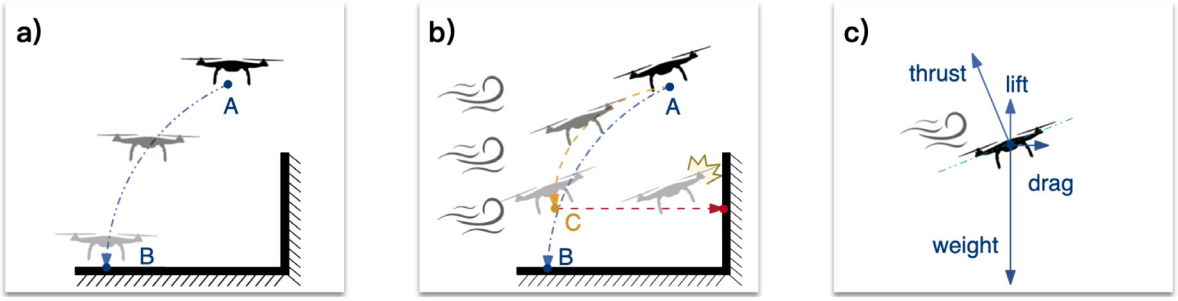

Fig. 1. A motivating example: Aerial physical interaction. (a) Without wind. (b) With wind. (c) Forces under the hover mode. In Fig. 1(a) and (b), A is the initial position, B is the target position, and C is the critical point. Suppose that the operator plans to let the drone safely move from points A to B, following an optimal trajectory given in Fig. 1(a), but the unexpected strong wind exists. Physically, the drone should face the wind and generate suitable thrust to compensate for the wind (drag) and gravity, as shown in Fig. 1(c). Note that the attitude (roll) and thrust should be kept within safe ranges. However, once the drone begins to descend, its thrust vector should be decreased and tilted, but there could not be enough force to compensate for the wind, which implies that the drone may be blown away or even crashed, as shown by Fig. 1(b). Hence, the "best performance" that can be achieved with the heavy wind is to stay in a critical point C, which may be far away from the target position B, with the suitable attitude and thrust to just compensate for the wind and gravity.

still an open problem to provide solutions without being too conservative. The first category is to further enhance a pre-designed nominal controller whose performance is robust against certain uncertainties. Methods under this category generally have the attractive property of an add-on patch, i.e., still keeping the well-tuned nominal controller but with an additional mechanism to modify the control input once any constraint becomes active. One classical approach under this category is the reference governor (RG, see Garone, Di Cairano, and Kolmanovsky (2017) and Kolmanovsky, Garone, and Di Cairano (2014) for detailed surveys and recent successful applications in safe human–robot coexistence (Merckaert et al., 2020) and legged robots control (Bratta et al., 2022)). In the framework of RG, a low-level controller is designed to robustly stabilise the system and an add-on filter for reference is designed to ensure constraint satisfaction. The recursive feasibility of RG can be guaranteed due to the robust invariance of the admissible set, however, the fact that only one-step prediction in the future is required to satisfy constraints may lead to poor performance (Rossiter & Kouvaritakis, 1998). Although RG is promising in safety-critical systems, it may be not suitable for the scenario where disturbances make a significant impact on the performance, e.g., see Fig. 1. As its name suggested, RG often assumes that constraint violations are caused by the change from the reference, and hence, its output admissible set is calculated for all the possible disturbances in a given set (Kolmanovsky et al., 2014, Sec. 2), which fails to fully exploit disturbances.

Another prominent method belongs to the first category is based on the control barrier function (CBF) (Ames, Xu, Grizzle, & Tabuada, 2016), which has been widely applied in robotics (Farzan, Azimi, Hu, & Rogers, 2022; Ferraguti et al., 2022). The safety condition described by the CBF with a well-defined relative degree, together with the stability condition described by the control Lyapunov function (CLF), are both regarded as the add-on constraints on the pre-designed nominal controller (Ames et al., 2019). The CBF-CLF-based safety framework is flexible as it can incorporate both the box constraints and the state-function ones, which, however, may bring considerable difficulties in guaranteeing the feasibility. Only a few works have been proposed to explore the feasibility, even for the pure CBF constraints, e.g., Xu (2018) and Xiao, Belta, and Cassandras (2022). The conditions on the feasibility-guaranteed CLF constraints remain unsolved mainly due to the lack of a general CLF construction method. The practical approach to the feasibility of CLF is to introduce a relaxation variable during optimisation (Ames et al., 2019; Ames et al., 2016), which may be unavoidably large and break the performance of the pre-designed convergence. Recent works considering the safety problem under the unknown environment have been focused on modifying either the nominal controller (Yan, Liu, Oh, & Chen, 2021) or the CBF using the disturbance estimate (Daş & Murray, 2022; Wang & Xu, 2022).

Different from the first kind of method, the second category directly formulates the control problem into a constrained optimisation without any hidden nominal controller. Among those, a widely-used method is model predictive control (MPC); this method has seen significant success in recent decades from the conventional process control to robotics (Corsini et al., 2022; Incremona, Ferrara, & Magni, 2017; Lindqvist, Mansouri, Aghamohammadi, & Nikolakopoulos, 2020), and has established itself as the primary control method for handling system constraints with several promising properties, e.g., guarantee of recursive feasibility and asymptomatic stability (Rawlings, Mayne, & Diehl, 2017). Due to its explosive growth, readers are directed to Mayne (2014) and Mayne, Rawlings, Rao, and Scokaert (2000) for detailed surveys; here we only focus on MPC design with the requirement of reference tracking while explicitly considering disturbance rejection. In order to obtain the offset-free tracking, appropriately embedding the model of the reference and the disturbance is necessary based on the well-known internal model principle (Isidori, 1995). Several early works have established a popular setup, generally named as the disturbance model formulation (Maeder, Borrelli, & Morari, 2009; Pannocchia & Bemporad, 2007; Pannocchia & Rawlings, 2003). This setup regards the current disturbance estimate as an initial state in the prediction model and lets the predicted disturbance in the horizon follow a given model. Several variants of offset-free MPC exist, e.g., the disturbance observer approach (Tatjewski, 2014) and the velocity form approach (Betti, Farina, & Scattolini, 2013), but they all show strong similarities with the disturbance model formulation (Pannocchia, 2015; Pannocchia, Gabiccini, & Artoni, 2015). Recent years have witnessed the wide adaptation of this setup in robotics applications which require high-precision tracking (Carron et al., 2019; Huang, Hofer, & D'Andrea, 2021; Liu, Chen, & Andrews, 2012). However, establishing theoretical conditions for this setup is very challenging because of the combined presence of state/disturbance observer, target calculation and receding-horizon optimisation. Indeed, almost all available methods for offset-free MPC follow a *static* analysis, i.e., assuming that the system can reach an asymptotically stable equilibrium, and then proving that offset-free control is attained at such an equilibrium (Maeder et al., 2009; Pannocchia, 2015; Pannocchia & Bemporad, 2007; Pannocchia et al., 2015; Pannocchia & Rawlings, 2003; Tatjewski, 2014). However, this static analysis cannot well guarantee the dynamic convergence, and easily

loses the recursive feasibility when the reference or disturbance changes (Rawlings et al., 2017; Rossiter, 2006). Towards the feasibility issue of the changing reference, a sensible way to increase the optimisation dimensions by involving artificial state and input as additional decision variables is proposed in Rossiter (2006). Following this contribution, some works have been done in other similar contexts, e.g., Betti et al. (2013), Limon, Alvarado, Alamo, and Camacho (2008), Limon, Ferramosca, Alvarado, and Alamo (2018) and Simon, Lofberg, and Glad (2014), where Limon et al. (2008) creatively use a special algebraic equation to parameterise the steady state and input, which could further save the computing resources.

The challenge in guaranteeing the recursive feasibility of MPC under disturbances lies in the time-varying estimation errors and unpredictable disturbances. An intuitive idea is to take robustness into account for MPC design, for example using tube-based MPC (Chisci, Rossiter, & Zappa, 2001; Mayne, Seron, & Rakovic, 2005). This kind of MPC develops a connection between the above-mentioned two categories in the sense that the system is optimised around a pre-designed nominal trajectory with tightened constraints. Since the tube-based MPC design is analogous to the nominal one, there are only a few works on reference tracking or disturbance rejection. In Limon, Alvarado, Alamo, and Camacho (2010), the tracking MPC is designed based on a nominal model, where all the disturbances in the original system are ignored. This approach is relatively conservative in the tube design as it has to cover all the possible realisation of the disturbance. In Xie, Dai, Lu, and Xia (2021), a feed-forward component is designed first based on the disturbance estimate in order to compensate for the external disturbance as much as possible; a stabilising MPC is then designed with the tube, which is only needed to cover the uncompensated disturbance and disturbance estimation error. Although recursive feasibility can be guaranteed by these methods, disturbances are all regarded as deleterious things to the control performance, and hence, are rejected intuitively, rather than being fully exploited.

1.3. Contributions

In this paper, we propose a novel optimal safety-critical control strategy for disturbed dynamic systems with the guarantee of safety and stability. The proposed method follows a natural and intuitive idea: Primarily keep the system in a *static* and *safe* equilibrium, and then cautiously drive the equilibrium to the given target as close as possible. To realise the first half of the idea, learning from disturbances will be required. The disturbance observer provides an estimation approach for the unknown disturbance. Here, we adopt only an original version of disturbance observer (DOB) (Chen, Ballance, Gawthrop, & O'Reilly, 2000), which can achieve asymptotic estimation when the disturbance is constant, but pay more attention to fully exploiting the disturbance estimate.

The contributions of this paper are threefold. As the main contribution, this paper provides a unified framework of safety-critical control design with the intervention from disturbances. From a high-level view, the proposed framework fully exploits the opportunities raised by disturbances. Disturbance estimate is not only used to improve the tracking accuracy as the conventional compensation-based approaches (Chen, Yang, Guo, & Li, 2015; Sariyildiz, Oboe, & Ohnishi, 2019) but also acts as a monitor to examine whether the current disturbance can be fully rejected. To obtain the condition on disturbance rejection of safety-critical systems, this paper shifts the focus from the disturbance side to the output reachability by defining a disturbance estimate-based output admissible (DEOA) set. Once the given reference exceeds the DEOA set (which implies that rejecting the current disturbance is a risky decision), the proposed method will transfer the objective of fully rejecting the disturbance into optimally coexisting with the disturbance.

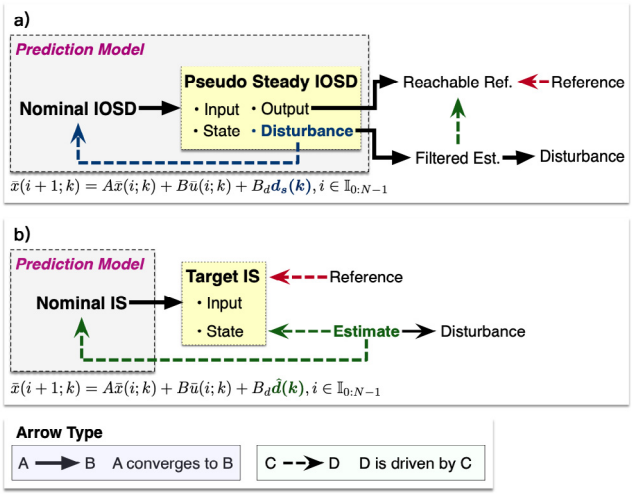

Fig. 2. Different setups in the tracking MPC. (a) The proposed method: A pseudo steady disturbance-based prediction. (b) The conventional method: A disturbance estimate-based prediction.

Another contribution is that this paper guarantees recursive feasibility for the first time when the disturbance estimate is involved in online optimisation, with the mild assumption that the external disturbance and its changing rate are bounded. To well demonstrate this contribution, we illustrate the setups of tracking MPC in Fig. 2, explicitly compared with the conventional offset-free MPC (Rawlings et al., 2017, Chaps. 1.5 and 5.5). In this paper, the recursive feasibility is guaranteed by embedding the quartet of pseudo steady input, output, state, and disturbance (IOSD) into optimisation. Note that as shown in Fig. 2(a), the prediction model here is online optimised and driven by a decision variable, the pseudo steady disturbance, rather than the disturbance estimate as in the conventional offset-free MPC. Hence, we are able to decouple the prediction model from the rapid change of disturbance estimates, which significantly contributes to the guarantee of recursive feasibility or safety. In contrast to the proposed method, as clearly stated in Rawlings et al. (2017, Page 356, Chap. 5.5.3), recursive feasibility of the conventional offset-free MPC can only be guaranteed in fairly limited scenarios, i.e., when the changing rate of estimation dynamics is sufficiently slow.

As a by-product, the last contribution lies in that this paper establishes a separation principle between the estimation and state feedback designs. In the context of the proposed MPC design, only the robustly asymptotic stability (RAS) set of estimation error would affect the tube computation, which implies that the proposed method not only copes with the peak phenomenon of high-gain observer (El Yaagoubi, El Assoudi, & Hammouri, 2004; Wang, Zuo, Wang, Yang, & Hu, 2022), but also renders the freedom of using a variety of estimation approaches. Besides, due to the reduced-order DOB and disturbance error-based tube design, the proposed method is initialisation-free, i.e., it works for any possible initial state of disturbance estimate, which may not be achieved by most existing methods. In the conventional output MPC, the initial estimation error is required to be within a pre-designed tube (Rawlings et al., 2017, Chap. 5); however, since that disturbance is unknown, this initial guess on the disturbance is generally difficult in practice or has to be quite conservative to be satisfied, otherwise an inappropriate initial guess may make the optimisation problem infeasible at the beginning.

Table 1
The frequently used sets and variables.

$\mathbb{X}$, $\mathbb{U}$	State and input constraints, (1)
$\bar{\mathbb{X}}$, $\bar{\mathbb{U}}$	Tightened state and input constraints, (16)
$\bar{\mathbb{X}}_f(\cdot)$	Terminal (state) set, (16)
$\mathbb{X}_s$, $\mathbb{U}_s$	Steady state and input set, (21)
$\mathbb{Y}_s(\cdot)$	Disturbance estimate-based output admissible set, (9)
$\mathbb{D}_1$, $\mathbb{D}_2$	Disturbance and its changing rate sets, (2)
$\mathbb{D}_L$	Robustly asymptomatic stability set of disturbance estimation error, (5)
$\mathbb{S}_K$	Robustly positive invariant set of disturbance error, (15)
$\mathbb{D}_s$	Steady disturbance (estimate) set, (6)
$\mathbb{P}_{(\cdot)}$	Optimisation problems, e.g., $\mathbb{P}_d$ in (7), $\mathbb{P}_r$ in (10), $\mathbb{P}_N$ in (14), and $\mathbb{P}_s$ in (24)
$(\cdot)_s$	Pseudo steady variables, e.g., u_s, y_s, x_s, d_s in (14)
$\hat{(\cdot)}$	Estimated variables, e.g., $\hat{d}$ in (4)
$c_{(\cdot)}$ or $(\cdot)_c$	Constants, e.g., c_r in (11) and d_c, r_c in Theorem 18
$(\cdot)^0$	Optimal variables for static optimisation problem, e.g., d_f^0 in (7) and r_f^0 in (10)
$(\cdot)^*$	Optimal variables for MPC optimisation problem, e.g., $\bar{x}^*$ and $\bar{u}^*$ in (14)

1.4. Organisation, notation and common definitions

The remainder of this paper is organised as follows. In Section 2, the control objective is first presented and followed by sufficient conditions on disturbance survival and rejection, which provide preliminaries for the proposed MPC framework in Section 3. The theoretical analysis on recursive feasibility and stability, and the numerical example are also provided in Section 3. The method developed in the paper is illustrated by an aerial physical interaction problem with experiments reported in Section 4. Finally, conclusions are provided in Section 5 and main proofs are located in Appendix A and Appendix B for the sake of readability.

Notation: $\mathbb{I}$ and $\mathbb{R}$ are integers and real numbers, respectively, where superscripts or subscripts may be added to give specific ranges. A C-set is a convex, compact set containing the origin. Consider $a \in \mathbb{R}^n$ and $b \in \mathbb{R}^m$, then $\text{col}(a, b) := [a^T, b^T]^T$; for a set $\Gamma \subset \mathbb{R}^{n+m}$, the projection of Γ onto a is defined as $\text{Proj}_a(\Gamma) := \{a \in \mathbb{R}^n \mid \exists b \in \mathbb{R}^m, \text{col}(a, b) \in \Gamma\}$. Given two sets $\mathbb{A} \subset \mathbb{R}^n$ and $\mathbb{B} \subset \mathbb{R}^n$, several basic set algebra operators are defined by $\mathbb{A} \oplus \mathbb{B} := \{a + b \mid a \in \mathbb{A}, b \in \mathbb{B}\}$, $\mathbb{A} \ominus \mathbb{B} := \{a \mid a \oplus \mathbb{B} \subseteq \mathbb{A}\}$ and $K\mathbb{A} := \{Ka \mid a \in \mathbb{A}\}$ where $K \in \mathbb{R}^{m\times n}$. Given a set $\mathbb{X} \subset \mathbb{R}^n$, we define its complement as $\mathbb{X}^\complement := \mathbb{R}^n \setminus \mathbb{X}$. The matrices $0_{n\times m} \in \mathbb{R}^{n\times m}$ and $I_n \in \mathbb{R}^{n\times n}$ denote a zero matrix and an identity matrix, respectively. For any matrix $A \in \mathbb{R}^{n\times n}$, $\rho(A)$ denotes the spectral radius. For any vector $x \in \mathbb{R}^n$, $|x|$ denotes the 2-norm and $|x|_P^2$ is defined by $|x|_P^2 := x^T P x$, where $P \in \mathbb{R}^{n\times n}$ is a symmetric matrix. For readability, the frequently used sets and variables in this paper are listed in Table 1.

The following definitions on robustly positive invariant (RPI) set (Rawlings et al., 2017, Page 217, Defin. 3.7) and robustly asymptotic stable (RAS) set (Rawlings et al., 2017, Page 230, Defin. 3.11) are useful in the design and analysis of this paper.

Definition 1. A set $\mathbb{S}$ is robustly positive invariant for system $x^+ = f(x, w),\ w \in \mathbb{W}$ if, for every $x \in \mathbb{S}$, $f(x, \mathbb{W}) \subseteq \mathbb{S}$.

Definition 2. Suppose the sets $\mathbb{S}_1$ and $\mathbb{S}_2$, $\mathbb{S}_1 \subset \mathbb{S}_2$, are robustly positive invariant for system $x^+ = f(x, w),\ w \in \mathbb{W}$. The set $\mathbb{S}_2$ is robustly asymptotic stable for $x^+ = f(x, w)$ in $\mathbb{S}_1$ if there exists a $\mathcal{KL}$ function $\beta(\cdot)$ such that every solution $\phi(\cdot; x, \mathbf{w})$ of $x^+ = f(x, w)$ with initial state $x \in \mathbb{S}_1$ and any disturbance sequence $\mathbf{w} \in \mathbb{W}^\infty$ satisfies $H(\phi(i; x, \mathbf{w}), \mathbb{S}_2) \le \beta(H(x, \mathbb{S}_2), i),\ \forall i \in \mathbb{I}_{\ge 0}$, where i is the time index and $H(x, \mathbb{S}_2) := \inf_{y\in\mathbb{S}_2} |x - y|$.

2. Problem formulation

2.1. System model

Consider a discrete-time system of the form:

$$\begin{aligned} x(k+1) &= Ax(k) + Bu(k) + B_d d(k) \\ y(k) &= Cx(k) \end{aligned} \tag{1}$$

where $x(k) \in \mathbb{R}^n$ is the state; $u(k) \in \mathbb{R}^m$ is the control; $y(k) \in \mathbb{R}^p$ is the output; and $d(k) \in \mathbb{R}^{n_d}$ is the unknown disturbance; $k \in \mathbb{I}_{\ge 0}$ is the current time, which may be skipped without causing ambiguity. The full state is measurable and the state and input trajectories are subject to the constraint $(x(k), u(k)) \in \mathbb{X} \times \mathbb{U}$, where both $\mathbb{X}$ and $\mathbb{U}$ are known C-sets, representing the state and input constraints, respectively. The initial state satisfies $x(0) \in \mathbb{X}$. The disturbance is assumed to satisfy the following assumption.

Assumption 3. The disturbance and its changing rate are bounded by:

$$d(k) \in \mathbb{D}_1,\ \ \Delta d(k) \in \mathbb{D}_2,\ \ \forall k \in \mathbb{I}_{\ge 0} \tag{2}$$

where $\Delta d(k) := d(k+1) - d(k)$; $\mathbb{D}_1$ and $\mathbb{D}_2$ are known C-sets.

The objective of this paper is to design a composite controller $u(k) = \kappa_N(x(k), \hat{d}(k), r(k))$ with a well-designed disturbance estimate $\hat{d}(k)$ and a given reference $r(k)$ such that the controlled plant:

$$x(k+1) = Ax(k) + B\kappa_N\left(x(k), \hat{d}(k), r(k)\right) + B_d d(k) \tag{3}$$

survives all disturbances satisfying Assumption 3. Furthermore, for any specific disturbance, the proposed controller will take every opportunity to fully reject it. To make the control objective clearer, we describe three different levels of interaction between the plant and the disturbance, whose definitions are given as follows.

Definition 4. Consider system (1) under the disturbance satisfying Assumption 3.

(1) Disturbance Survival: For a given disturbance $d(k)$, if the safety constraint $(x(k), u(k)) \in \mathbb{X} \times \mathbb{U},\ k \in \mathbb{I}_{\ge 0}$ is always fulfilled, system (1) is said to survive disturbance $d(k)$. If system (1) survives all possible disturbance realisations satisfying Assumption 3, system (1) is said to survive all disturbances.
(2) Disturbance Rejection: For a given disturbance $d(k)$, if the proposed controller is able to steer the output $y(k)$ to the given reference $r(k)$ and system (1) survives disturbance $d(k)$, disturbance $d(k)$ is said to be fully rejected.
(3) Disturbance Optimal Coexistence: For a given disturbance $d(k)$, if the proposed controller is able to steer the output $y(k)$ to an optimal solution corresponding to a predefined performance index, but fails to fully reject disturbance $d(k)$, and system (1) survives disturbance $d(k)$, system (1) is said to optimally coexist with disturbance $d(k)$.

Here, reference $r(k)$ is assumed to be unknown in advance, representing an input from human operator or a high-level decision making.

Remark 5. Disturbance survival, rejection, and optimal coexistence are all important aspects of safety-critical control systems, with emphasis on the intervention from disturbance. Disturbance survival refers to the satisfaction of safety constraints throughout the entire duration of system operation under all possible disturbance realisations. On the other hand, disturbance rejection

further requires the objective to be achieved eventually, such as offset-free tracking to the given reference under the specific disturbance. Optimal coexistence is a compromised status when disturbance rejection cannot be safely achieved.

2.2. Disturbance estimation filter

Since disturbance $d(k)$ is unknown, it is necessary to estimate it first. Although multiple types of disturbance observers exist with different features (Chen et al., 2015; Sariyildiz et al., 2019), we follow only an original version (Chen et al., 2000) but focus more on the approach of embedding the disturbance estimate into optimisation. The DOB is designed as follows:

$$z(k+1) = (I_{n_d} - LB_d)z(k) + (L - LA - LB_dL)x(k) - LBu(k) \tag{4a}$$

$$\hat{d}(k) = z(k) + Lx(k) \tag{4b}$$

where $L \in \mathbb{R}^{n_d \times n}$ is the observer gain; $z(k) \in \mathbb{R}^{n_d}$ is the auxiliary variable; $\hat{d}(k) \in \mathbb{R}^{n_d}$ is the disturbance estimate. Given that the asymptotic estimation in (4) is only applicable to constant disturbances, it is reasonable to expect that effective disturbance rejection can only be achieved under the same condition.

Define the disturbance estimation error as $\tilde{d}(k) := d(k) - \hat{d}(k)$. Taking DOB (4) into plant (1) yields the following estimation error system:

$$\tilde{d}(k+1) = A_L\tilde{d}(k) + \Delta d(k) \tag{5}$$

where $A_L := I_{n_d} - LB_d$. Suppose that there exists an observer gain L such that A_L is stable, i.e., $\rho(A_L) < 1$, system (5) is input-to-state stable (ISS) with respect to $\Delta d(k) \in \mathbb{D}_2$. Then robustly asymptotic stability (RAS) set $\mathbb{D}_L$ exists for the estimation error $\tilde{d}(k)$. That is, there exists a time instant k_1 such that $\tilde{d}(k) \in \mathbb{D}_L$ holds for all $k \geq k_1$. In other words, $\hat{d}(k)$ will be captured by its steady set

$$\mathbb{D}_s := \mathbb{D}_1 \oplus (-\mathbb{D}_L), \tag{6}$$

i.e., $\hat{d}(k) \in \mathbb{D}_s$ holds for all $k \geq k_1$.

It is worth noting that even a small initial error $\tilde{d}(0)$ may lead to a large estimation error due to the pursuit of faster estimation performance. If the disturbance estimate is directly into the closed-loop system, then it will yield a peak error on the system or even break the safety (El Yaagoubi et al., 2004; Wang et al., 2022). To avoid this peak phenomenon, we design the following optimisation problem:

$$\mathbb{P}_d\left(\hat{d}\right): \ d_f^0 := \arg\min_{d_f \in \mathbb{D}_s} \left| d_f - \hat{d} \right|^2. \tag{7}$$

The optimisation problem $\mathbb{P}_d(\hat{d})$ generally acts as a saturation function for the disturbance estimate: Once the disturbance estimate is out of the steady disturbance set $\mathbb{D}_s$, it will return the closest one on the boundary of $\mathbb{D}_s$.

Remark 6. A common way to construct the RAS set $\mathbb{D}_L$ for the estimation error dynamics is using the sub-level set of the Lyapunov function of system (5). Readers can refer to Jiang and Wang (2001, Lemma 3.5) for the detailed construction approach.

2.3. Interactions with disturbances

With the filtered disturbance estimate, we are now able to give several sufficient conditions on surviving and rejecting disturbances, which are based on the steady state and input sets, $\mathbb{X}_s \subseteq \mathbb{X}$ and $\mathbb{U}_s \subseteq \mathbb{U}$. These two sets, $\mathbb{X}_s$ and $\mathbb{U}_s$, are defined as the ranges of the current state x and input u that guarantee the system exhibits a static behaviour for all possible disturbances $d \in \mathbb{D}_s$, which facilitate the construction of trackable reference and stability analysis. Here, the steady disturbance set $\mathbb{D}_s$ is used instead of the real disturbance set $\mathbb{D}_1$ in order to capture the effect of disturbance estimation error. The steady sets $\mathbb{X}_s$ and $\mathbb{U}_s$ will be specifically constructed in Section 3.3.

2.3.1. Disturbance survival

The condition of surviving disturbances is inspired by the aerial physical interaction scenario in Fig. 1, especially the drone stays statically in the critical point under the strong wind. Hence, the system is desired to reach a dynamic equilibrium under all possible realisations of disturbances. It is also quite necessary, since if the steady state and input are not able to survive all disturbances, the system will be either oscillating within the safety region or "blown away" and break the safety requirement, as seeing the drone crash case in Fig. 1(b). Both consequences are not acceptable in practice. Such a consideration can be geometrically formulated by Assumption 7, which is proved to be sufficient for surviving all disturbances in Lemma 8.

Assumption 7. The steady state, input and disturbance sets satisfy the following relation:

$$(A - I_n)\mathbb{X}_s \oplus B\mathbb{U}_s \supseteq -B_d\mathbb{D}_s. \tag{8}$$

Lemma 8. *System (1) survives all disturbances, if condition (8) holds.*

Proof. Noting that $\mathbb{D}_2$ is a C-set, we have that $\mathbb{D}_L$ contains the origin, which implies that $\mathbb{D}_s \supseteq \mathbb{D}_1$. Suppose that (8) holds, then for any disturbance $d \in \mathbb{D}_1 \Rightarrow -B_dd \in -B_d\mathbb{D}_1 \subseteq -B_d\mathbb{D}_s$, there exists a pair of $(x, u) \in \mathbb{X}_s \times \mathbb{U}_s \subseteq \mathbb{X} \times \mathbb{U}$ such that $(A - I_n)x + Bu = -B_dd$. Thus, $x^+ = x \in \mathbb{X}_s \subseteq \mathbb{X}$. Hence, the safety constraint $(x(k), u(k)) \in \mathbb{X} \times \mathbb{U}$, $k \in \mathbb{I}_{\geq 0}$ is always fulfilled for all possible disturbance realisations satisfying Assumption 3, which completes the proof. ■

Remark 9. Assumption 7 is consistent with the feasibility requirement of the target calculation in offset-free MPC (Rawlings et al., 2017, Chap. 5.5) when the disturbance estimate is bounded within a given set $\mathbb{D}_s$. However, it is important to note that Assumption 7 provides a pre-design verification criterion that establishes a safe operating envelope. As demonstrated later in Theorem 16, this assumption is critical for achieving recursive feasibility (safety). Besides, the verification process is straightforward since the construction of the steady constraints $\mathbb{X}_s$ and $\mathbb{U}_s$ is completely independent of any disturbance-related variables, as explained in Section 3.3. Additionally, based on the definition of disturbance steady set $\mathbb{D}_s$, Assumption 7 implicitly includes the requirements on disturbance sets $\mathbb{D}_1$ and $\mathbb{D}_2$.

2.3.2. Disturbance rejection and towards optimal coexistence

By Definition 4, a disturbance can be fully rejected if the reference can be tracked, which implies that the reachability of output is significant for examining disturbance rejection. We first define the output admissible set, which is named as disturbance estimate-based output admissible (DEOA) set to emphasise that we take full use of the disturbance information and distinguish it from the definition in reference governor (RG)-based methods.

Supposing that Assumption 7 holds, for any given disturbance $d_s \in \mathbb{D}_s$, there must exist at least a pair of (x_s, u_s) satisfying that $(A - I_n)x_s + Bu_s = -B_dd_s$. Then, we can define the DEOA set as follows:

$$\mathbb{Y}_s(d_s) := \Big\{ y_s = Cx_s \mid (A - I_n)x_s + Bu_s = -B_dd_s, \\ x_s \in \mathbb{X}_s, u_s \in \mathbb{U}_s \Big\} \subseteq C\mathbb{X}_s. \tag{9}$$

With the DEOA set (9), we can deduce a sufficient condition for rejecting disturbance.

Lemma 10. *Disturbance d is fully rejected, if condition $r \in \mathbb{Y}_s(d)$ holds.*

Proof. Suppose that $r \in \mathbb{Y}_s(d)$, then there exists a pair of $(x, u) \in \mathbb{X}_s \times \mathbb{U}_s \subseteq \mathbb{X} \times \mathbb{U}$ such that both $(A - I_n)x + Bu = -B_d d$ and $y = Cx = r$ hold. Similarly, we have $x^+ = x$ and $y^+ = y = r$. This completes the proof. ■

Towards optimal coexistence with disturbances, once the reference is out of DEOA, a cautious way is to generate a reachable or trackable reference for the system to follow, which is the closest admissible target under the current disturbance estimate. We then design the following optimisation problem:

$$\mathbb{P}_r\left(d_f^0, r\right): \; r_f^0 := \arg \min_{r_f \in \mathbb{Y}_s\left(d_f^0\right)} \left|r_f - r\right|^2. \tag{10}$$

It is worth noting that the approach to determine the reachable reference is extendable to consider the changing rate of reachable reference to avoid oscillation.

Assumption 11. For a given reference r, there exists a constant $c_r > 0$ such that

$$\left|r_{f1}^0 - r_{f2}^0\right| \le c_r \left|d_{f1}^0 - d_{f2}^0\right| \tag{11}$$

holds, if $d_{f1}^0 \in \mathbb{D}_s$ and $d_{f2}^0 \in \mathbb{D}_s$ are arbitrarily close, where r_{f1}^0 and r_{f2}^0 are the optimal solutions of $\mathbb{P}_r(d_{f1}^0, r)$ and $\mathbb{P}_r(d_{f2}^0, r)$, respectively.

Remark 12. Noting that the DEOA set $\mathbb{Y}_s(\cdot)$ in (10) is the function of d_f^0 and if the difference between d_{f1}^0 and d_{f2}^0 is arbitrarily small, the difference between the boundaries of $\mathbb{Y}_s(d_{f1}^0)$ and $\mathbb{Y}_s(d_{f2}^0)$ would also be arbitrarily small, so will be the difference between r_{f1}^0 and r_{f2}^0. This geometric interpretation is depicted in Fig. 3, where a first-order example is considered. Assumption 11 is a mathematical expression on the above-mentioned observation and is in the form of local Lipschitz continuity for convenience in the subsequent stability analysis. Besides, it is worth noting that we only assume the existence of the Lipschitz constant c_r, but without any limitation on its size; the Lipschitz constant c_r is independent of the following design process, which only affects the construction of the Lyapunov function $W(k)$. Furthermore, if polyhedral sets are considered here, (10) can be transformed into a multi-parametric quadratic programming (mp-QP) problem with the parameter d_f^0 appearing only on the right-hand side of the constraints. Under mild conditions, r_f^0 is continuous and piecewise affine with respect to d_f^0 (Bemporad, Morari, Dua, & Pistikopoulos, 2002, Sec. 4), which also naturally verifies Assumption 11. The detailed process using the mp-QP formulation has been provided in Appendix C.

3. Augmented predictive control framework

To obtain the control objective, *surviving all disturbances but taking every opportunity to reject them*, a new tracking MPC framework is proposed under the name *augmented predictive control* (APC), which emphasises not only the hierarchical structure but also the augmented dimensions of optimisation. Before presenting the detailed design, the overall control scheme is given by Fig. 4, where the control input applied to the system (1) is still following a classical format, that is:

$$u(k) := K\left(x(k) - \bar{x}^*(0;k)\right) + \bar{u}^*(0;k) \tag{12}$$

where K is the controller gain, which needs to let $A_K := A + BK$ be stable, i.e., $\rho(A_K) < 1$; the given reference and disturbance estimate are in-explicitly contained in the optimal nominal state $\bar{x}^*(0;k)$ and input $\bar{u}^*(0;k)$.

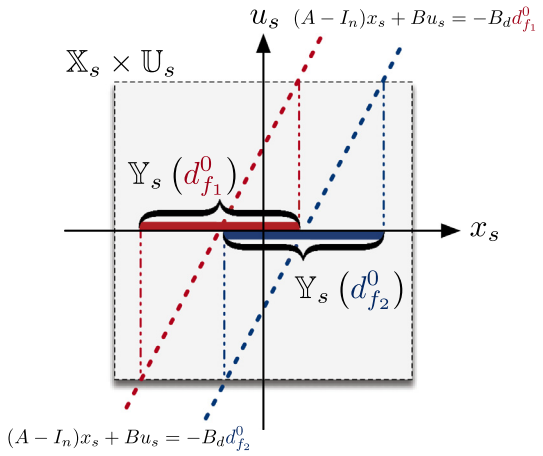

Fig. 3. A geometric interpretation of Assumption 11, where $A = -1$, $B = B_d = C = 1$ and $\mathbb{U}_s = \mathbb{X}_s = [-1, 1]$. Two auxiliary lines are drawn, corresponding to different disturbances $d_{f_1}^0$ and $d_{f_2}^0$, respectively. To verify the validity of Assumption 11, three cases need to be considered: (1) $r \in \mathbb{Y}_s(d_{f_1}^0) \cap \mathbb{Y}_s(d_{f_2}^0)$, (2) $r \in \mathbb{Y}_s^c(d_{f_1}^0) \cap \mathbb{Y}_s^c(d_{f_2}^0)$, and (3) $r \in \mathbb{Y}_s^c(d_{f_1}^0) \cap \mathbb{Y}_s(d_{f_2}^0)$ or $r \in \mathbb{Y}_s(d_{f_1}^0) \cap \mathbb{Y}_s^c(d_{f_2}^0)$.

3.1. Main results

We are now in a position to specify the new optimisation problem, whose solution yields the optimal steady input, output, state, disturbance (IOSD), and nominal state and input. The proposed cost function is given as follows, which is a combination of the cost function from the conventional tracking MPC and the penalties on the error between pseudo disturbance and disturbance estimate, and that between pseudo output and reference:

$$\begin{aligned} &V_N\left(\mathrm{IOSD}(k), \bar{\mathbf{u}}(k), \bar{x}(0;k), d_f^0(k), r_f^0(k)\right) \\ &:= \sum_{i=0}^{N-1} \ell\left(\bar{x}(i;k) - x_s(k), \bar{u}(i;k) - u_s(k)\right) + V_f(\bar{x}(N;k) - x_s(k)) \\ &\quad + V_d\left(d_f^0(k) - d_s(k)\right) + V_y\left(r_f^0(k) - y_s(k)\right) \end{aligned} \tag{13}$$

where

$$\ell(\bar{x}(i;k) - x_s(k), \bar{u}(i;k) - u_s(k)) := |\bar{x}(i;k) - x_s(k)|_Q^2 + |\bar{u}(i;k) - u_s(k)|_R^2$$

$$V_f(\bar{x}(N;k) - x_s(k)) := |\bar{x}(N;k) - x_s(k)|_P^2$$

$$V_d(d_f^0(k) - d_s(k)) := |d_f^0(k) - d_s(k)|_{P_d}^2$$

$$V_y(r_f^0(k) - y_s(k)) := |r_f^0(k) - y_s(k)|_{P_y}^2;$$

$\bar{x}(i;k)$ denotes the prediction obtained by iterating model i times from the initial state $\bar{x}(0;k)$; IOSD(k) denotes the pseudo steady sequence $(u_s(k), y_s(k), x_s(k), d_s(k))$; $\bar{\mathbf{u}}(k)$ denotes the control sequence $(\bar{u}(0;k), \bar{u}(1;k), \ldots, \bar{u}(N-1;k))$; N denotes the prediction horizon; Q, R, P, P_d, P_y are the positive definite weightings, and the terminal weighting P is designed to cover the cost-to-go and guarantee the stability.

The proposed APC is derived from the following optimisation problem:

$$\mathbb{P}_N\left(x, d_f^0, r_f^0\right): \min_{\mathrm{IOSD}(k), \bar{\mathbf{u}}(k), \bar{x}(0;k)} V_N(\cdot) \tag{14}$$

s.t.

$$\bar{x}(0;k) \in \{x(k)\} \oplus (-\mathbb{S}_K) \tag{14a}$$

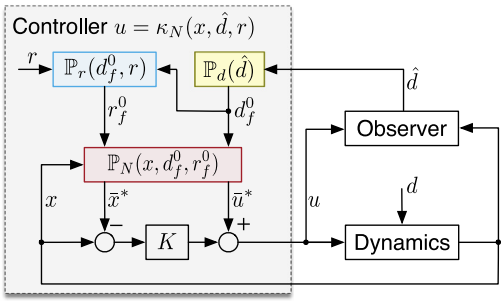

Fig. 4. Schematic of the proposed method.

$$\bar{x}(i+1;k) = A\bar{x}(i;k) + B\bar{u}(i;k) + B_d d_s(k) \tag{14b}$$

$$\bar{x}(i;k) \in \bar{\mathbb{X}},\ \bar{u}(i;k) \in \bar{\mathbb{U}},\ i \in \mathbb{I}_{0:N-1} \tag{14c}$$

$$\bar{x}(N;k) \in \bar{\mathbb{X}}_f(x_s(k)) \tag{14d}$$

$$\begin{bmatrix} A - I_n & B \\ C & 0_{p\times m} \end{bmatrix} \begin{bmatrix} x_s(k) \\ u_s(k) \end{bmatrix} = \begin{bmatrix} -B_d d_s(k) \\ y_s(k) \end{bmatrix} \tag{14e}$$

$$x_s(k) \in \mathbb{X}_s,\ u_s(k) \in \mathbb{U}_s,\ d_s(k) \in \mathbb{D}_s \tag{14f}$$

where $\mathbb{S}_K$ denotes the uncertainty set containing all possible realisations of estimation errors; $\bar{\mathbb{X}}$ and $\bar{\mathbb{U}}$ denote the tightened constraints for state and input; $\bar{\mathbb{X}}_f(x_s(k))$ denotes the terminal constant, which depends on the current pseudo steady state; $\mathbb{X}_s$ and $\mathbb{U}_s$ are the steady sets of state and input. Several undefined sets will be specified subsequently.

3.2. Disturbance error-based tube design

In this section, we will focus on the specific design for the tube $\mathbb{S}_K$ in (14a) and the tightened constraints $\bar{\mathbb{X}}$ and $\bar{\mathbb{U}}$ in (14c).

The motivation to use the tube here is mainly due to the difference between the real disturbance and the pseudo steady disturbance during the optimisation. Although we can expect that the error between these two would converge to zero under the mild assumption, the initial error is unpredictable due to the unknown disturbance. Hence, a worst-case design has to be considered. Let $e(0;k) := x(k) - \bar{x}(0;k)$ and $e(1;k) := x(k+1) - \bar{x}(1;k)$. Subtracting (1) from (14b) will yield:

$$e(1;k) = A_K e(0;k) + B_d\left(d(k) - d_s(k)\right). \tag{15}$$

Noting that $d(k) - d_s(k) \in \mathbb{D}_1 \oplus (-\mathbb{D}_s) = \mathbb{D}_1 \oplus (-\mathbb{D}_1) \oplus \mathbb{D}_L$, we define $\mathbb{W}_L := B_d(\mathbb{D}_1 \oplus (-\mathbb{D}_1) \oplus \mathbb{D}_L)$. Let $\mathbb{S}_K$ be the robustly positive invariant (RPI) set for (15), i.e., $A_K\mathbb{S}_K \oplus \mathbb{W}_L \subseteq \mathbb{S}_K$, whose existence is guaranteed if A_K is stable (see Gilbert and Tan (1991, Sec.1) for further details). Then, we can define the tightened constraints as the conventional tube-based MPC:

$$\bar{\mathbb{X}} := \mathbb{X} \ominus \mathbb{S}_K,\ \bar{\mathbb{U}} := \mathbb{U} \ominus K\mathbb{S}_K. \tag{16}$$

In the optimisation problem $\mathbb{P}_N(x, d_f^0, r_f^0)$, the constraint (14a) forces the initial error $e(0;k)$ to be within the tube and due to the RPI property, we have $e(1;k) \in \mathbb{S}_K$, i.e., $\bar{x}(1;k) \in \{x(k+1)\} \oplus (-\mathbb{S}_K)$.

3.3. Steady and terminal constraints design

In this section, we will focus on the specific design for the terminal and steady state constraints $\bar{\mathbb{X}}_f$, $\mathbb{X}_s$ and $\mathbb{U}_s$ in (14d) and (14f).

The terminal condition designed here follows the spirit of the stabilising condition in the conventional MPC (Rawlings et al., 2017, Chap. 2.4). We first fix the format of the terminal controller as follows:

$$\bar{u}(N;k) = \bar{K}(\bar{x}(N;k) - x_s(k)) + u_s(k) \tag{17}$$

where $\bar{K}$ is the terminal controller gain. Taking (17) into the (14b) and keeping (14e) in mind will give:

$$\bar{x}(N+1;k) = A_{\bar{K}}(\bar{x}(N;k) - x_s(k)) + x_s(k) \tag{18}$$

where $A_{\bar{K}} := A + B\bar{K}$. It is worth noting that no disturbance information is involved in (18). Let $x_a(N;k) := \mathrm{col}(\bar{x}(N;k), x_s(k), u_s(k)) \in \mathbb{R}^{2n+m}$. The dynamics of the augmented system and the terminal controller are both obtained from (18), as follows:

$$x_a(N+1;k) = A_a x_a(N;k),\ \ \bar{u}(N;k) = [\bar{K}, -\bar{K}, I_m]x_a \tag{19}$$

where

$$A_a := \begin{bmatrix} A_{\bar{K}} & I_n - A_{\bar{K}} & 0_{n\times m} \\ 0_{n\times n} & I_n & 0_{n\times m} \\ 0_{m\times n} & 0_{m\times n} & I_m \end{bmatrix}.$$

An admissible invariant set $\Theta_{\bar{K}}$ for system (19) can be defined by:

$$A_a\Theta_{\bar{K}} \subseteq \Theta_{\bar{K}} \subseteq \mathbb{X}_a \tag{20}$$

where

$$\mathbb{X}_a := \left\{x_a \in \mathbb{R}^{2n+m} \mid x_a \in \bar{\mathbb{X}} \times \lambda\bar{\mathbb{X}} \times \lambda\bar{\mathbb{U}}, [\bar{K}, -\bar{K}, I_m]x_a \in \bar{\mathbb{U}}\right\}$$

and $\lambda \in (0,1)$ can be chosen arbitrarily close to 1.The introduction of λ in $\mathbb{X}_a$ is to obtain a finitely-determined approximation of the maximal admissible invariant set, which hence is convex (Gilbert & Tan, 1991). Besides, noting the identity matrices in the main diagonal of A_a, the invariant sets for steady state and input can be specified using the projection operation while the terminal set is related to the steady state and can be specified using a similar operation, as follows:

$$\begin{aligned} &\mathbb{X}_s := \mathrm{Proj}_{x_s}(\Theta_{\bar{K}}) \subseteq \lambda\bar{\mathbb{X}} \subset \bar{\mathbb{X}} \\ &\mathbb{U}_s := \mathrm{Proj}_{u_s}(\Theta_{\bar{K}}) \subseteq \lambda\bar{\mathbb{U}} \subset \bar{\mathbb{U}} \\ &\bar{\mathbb{X}}_f(x_s) := \left\{\bar{x}_N \in \mathbb{R}^n \mid \forall u_s \in \mathbb{U}_s, \mathrm{col}(\bar{x}_N, x_s, u_s) \in \Theta_{\bar{K}}\right\} \subseteq \bar{\mathbb{X}}, \\ &\qquad\qquad\qquad\qquad\qquad\qquad \forall x_s \in \mathbb{X}_s. \end{aligned} \tag{21}$$

With (21), it is geometrical to conclude that:

$$\Theta_{\bar{K}} = \bigcup_{x_s\in\mathbb{X}_s} \bar{\mathbb{X}}_f(x_s) \times \mathbb{X}_s \times \mathbb{U}_s \tag{22}$$

which can also be proved using the set contain relationship. Besides, $\mathbb{X}_s$ and $\mathbb{U}_s$ are both convex (Boyd, Boyd, & Vandenberghe, 2004, Chap. 2.3.2).

In the meantime, the terminal weighting P and its controller gain $\bar{K}$ can be easily obtained from the discrete algebraic Riccati inequality:

$$A_{\bar{K}}^T P A_{\bar{K}} - P + Q + \bar{K}^T R\bar{K} \le 0. \tag{23}$$

3.4. Optimisation-based steady IOSD discussion

In this section, we will discuss the optimisation-based approach to compute the steady IOSD in (14e) and show the differences with that in the conventional offset-free MPC.

To simplify the analysis, we consider a steady-state scenario where the tracking items in (13) are all set to zeros. Hence, $\mathbb{P}_N(x, d_f^0, r_f^0)$ will be simplified to the following optimisation problem:

$$\mathbb{P}_s\left(d_f^0, r_f^0\right): \min_{\text{IOSD}}\ V_d\left(d_f^0 - d_s\right) + V_y\left(r_f^0 - y_s\right) \tag{24}$$

$$\text{s.t.} \begin{bmatrix} A - I_n & B \\ C & 0_{p\times m} \end{bmatrix} \begin{bmatrix} x_s \\ u_s \end{bmatrix} = \begin{bmatrix} -B_d d_s \\ y_s \end{bmatrix} \tag{24a}$$

$$x_s \in \mathbb{X}_s,\ u_s \in \mathbb{U}_s,\ d_s \in \mathbb{D}_s. \tag{24b}$$

The proposed approach is meaningful in the sense that the optimal steady disturbance and output are exactly the same as the

given ones, i.e., d_f^0 and r_f^0. This inference is proved by Lemma 13 and will play a significant role in the stability analysis. On the other hand, it is worth noting that during the transition process, the optimised IOSD obtained from (13) only can serve as *pseudo steady* sequences.

Lemma 13. *Suppose that Assumption 7 holds, then the value function of $\mathbb{P}_s(d_f^0, r_f^0)$ is 0 and its partial optimal solutions are $d_s^0 = d_f^0$, $y_s^0 = r_f^0$.*

Proof. By the definition of $\mathbb{P}_r(d_f^0, r)$, i.e., $r_f^0 \in \mathbb{Y}_s(d_f^0)$, there exist $\tilde{x}_s \in \mathbb{X}_s$ and $\tilde{u}_s \in \mathbb{U}_s$ such that $(A - I_n)\tilde{x}_s + B\tilde{u}_s = -B_d\tilde{d}_s$, $C\tilde{x}_s = \tilde{y}_s$ where $\tilde{d}_s := d_f^0$ and $\tilde{y}_s := r_f^0$. Since that $(\tilde{u}_s, \tilde{y}_s, \tilde{x}_s, \tilde{u}_s)$ is a feasible solution of the optimisation problem $\mathbb{P}_s(d_f^0, r_f^0)$, taking the corresponding disturbance and output, $\tilde{d}_s$ and $\tilde{y}_s$, into the cost function will get $V_d(d_f^0 - \tilde{d}_s) + V_y(r_f^0 - \tilde{y}_s) = 0$. And hence, the value function of $\mathbb{P}_s(d_f^0, r_f^0)$ is 0. It also implies that the partial optimal solutions should satisfy that $d_s^0 = d_f^0$, $y_s^0 = r_f^0$ due to the optimality, which completes the proof. ■

Remark 14. It is worth noting that the external signals d_f^0 and r_f^0 are only involved in the cost function, rather than the constraints of the optimisation problem (24). This approach is completely different from the conventional offset-free MPC design, e.g., Maeder et al. (2009) and Rawlings et al. (2017, Chap. 5.5), where the disturbance and reference items are directly involved in the equation constraint. Once the disturbance (estimate) or the given reference is rapidly changed, the feasibility of the conventional offset-free MPC cannot be easily guaranteed, which would break the safety requirement (Limon et al., 2008, 2018; Simon et al., 2014).

Remark 15. Lemma 13 also implies the necessity of introducing the optimisation problem $\mathbb{P}_r(d_f^0, r)$. If one directly puts the reference r into the optimisation problem $\mathbb{P}_s(d_f^0, r_f^0)$, i.e., replacing the optimal reference r_f^0 by the given one r, the value function of $\mathbb{P}_s(d_f^0, r_f^0)$ cannot be zero if $r \notin \mathbb{Y}_s(d_f^0)$. This will lead to the optimal steady disturbance d_s^0 may not be the target one, d_f^0, which is desired to converge to the external disturbance d. Once the optimal steady disturbance cannot converge to the external disturbance, the optimal state and input will lose their physical meaning as they are not matched with the real ones under the current environment.

3.5. Algorithm implementation

Now, the proposed control algorithm can be formally stated as Algorithm 1. To clarify the algorithm, the signal flow is started from the disturbance estimate, which also corresponds to the control scheme shown in Fig. 4.

3.6. Theoretical analysis

The following theorems present the results on recursive feasibility and stability, whose proofs are located in Appendix A and Appendix B for the sake of readability.

Theorem 16. *Suppose that Assumptions 3 and 7 hold. Then, system (1) controlled by (12) always fulfils the safety constraints throughout the time, if the optimisation problem $\mathbb{P}_N(x(k), d_f^0(k), r_f^0(k))$ in (14) is feasible at the time $k = 0$.*

Assumption 17. The matrix

$$\begin{bmatrix} A - I_n & B \\ C & 0_{p\times m} \end{bmatrix}$$

is nonsingular.

Algorithm 1 Augmented Predictive Control

1: **Offline:** Specify the weightings Q, R, P, P_y, and P_d, prediction horizon N, controller and observer gains K and L, and constraints $\bar{\mathbb{X}}$, $\bar{\mathbb{U}}$, $\bar{\mathbb{X}}_f$, $\mathbb{X}_s$, $\mathbb{U}_s$, and $\mathbb{D}_s$. ▷ See Sec. 3.2 and Sec. 3.3.
2: **Initialise:** Set the time $k = 0$ and specify the observer state $z(0)$.
3: **Step One-Estimation Filter:**
   a) Measure the current state $x(k)$ and receive the observer state $z(k)$ to compute the disturbance estimate $\hat{d}(k)$ from (4b).
   b) Solve the static optimisation problem $\mathbb{P}_d(\hat{d}(k))$ in (7) to obtain $d_f^0(k)$. ▷ See Sec. 2.2.
4: **Step Two-Reachable Reference:** Receive the current reference $r(k)$. Solve the static optimisation problem $\mathbb{P}_r(d_f^0(k), r(k))$ in (10) to obtain $r_f^0(k)$. ▷ See Sec. 2.3.
5: **Step Three-Nominal State/Input:** Solve the nominal optimisation control problem $\mathbb{P}_N(x(k), d_f^0(k), r_f^0(k))$ in (14) to obtain $\bar{x}^*(0; k)$ and $\bar{u}^*(0; k)$. ▷ See Sec. 3.1.
6: **Step Four-Controller/Observer:**
   a) Compute the current controller $u(k)$ from (12) and apply it into system (1) to generate the successor state $x(k+1)$.
   b) Compute the successor estimate $z(k+1)$ from (4a).
   c) Set $k \leftarrow k+1$ and go to **Step One**.

Theorem 18. *Suppose that Assumptions 3, 7, and 11 hold, the optimisation problem $\mathbb{P}_N(x(k), d_f^0(k), r_f^0(k))$ in (14) is feasible at the time $k = 0$, and the disturbance and reference are constants in the steady state, i.e., $d(k) = d_c$, $r(k) = r_c$ hold for all $k \geq k_2$. Then,*

(1) If $r_c \in \mathbb{Y}_s(d_c)$, the control output $y(k)$ asymptotically converges to the set $\{r_c\} \oplus C\mathbb{S}_K$.
(2) If $r_c \notin \mathbb{Y}_s(d_c)$, the control output $y(k)$ asymptotically converges to the set $\{r_{fc}^0\} \oplus C\mathbb{S}_K$, where

$$r_{fc}^0 := \arg \min_{r_f \in \mathbb{Y}_s(d_c)} \left| r_f - r \right|^2 .$$

Further, suppose that Assumption 17 holds, then

(3) If $r_c \in \mathbb{Y}_s(d_c)$, the control output $y(k)$ asymptotically converges to r_c.
(4) If $r_c \notin \mathbb{Y}_s(d_c)$, the control output $y(k)$ asymptotically converges to r_{fc}^0.

Remark 19. Assumption 17 is quite general since it is the necessary and sufficient condition on existence of the feasible target (Rawlings et al., 2017, Lemma 1.14) once the dimensions of input are the same with that of output. Besides, if Assumption 17 holds, by using its inversion, the decision variable IOSD(k) in $\mathbb{P}_N(x, d_f^0, r_f^0)$ could be reduced to IS(k) or OD(k), which is the pseudo steady sequence of $(u_s(k), x_s(k))$ or $(y_s(k), d_s(k))$.

3.7. Numerical example

In this section, a numerical example is given to illustrate the effectiveness of the proposed method, especially when the disturbance cannot be fully rejected.

Consider a linear system given by:

$$A = \begin{bmatrix} 0.5 & 1 \\ 1 & 1 \end{bmatrix}, \; B = \begin{bmatrix} 0 & 1 \\ 1 & 0 \end{bmatrix}, \; B_d = \begin{bmatrix} 1 & 1 \\ 0 & 1 \end{bmatrix}, \; C = I_2$$

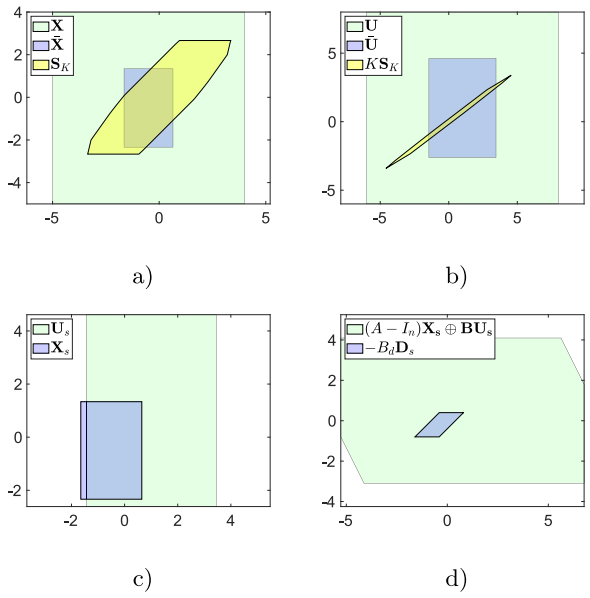

Fig. 5. Sets. (a) State tube. (b) Control tube. (c) Steady sets. (d) Disturbance set.

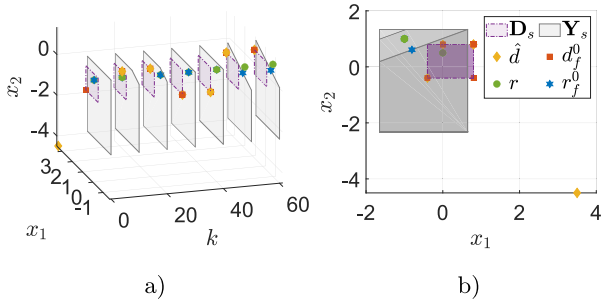

Fig. 6. Evolution of the DEOA set at the interval of 10 samples. (a) 3D view. (b) Front view.

with the state and input constraints $\mathbb{X} = [-5, 4]^2$, $\mathbb{U} = [-6, 8]^2$, and the disturbance range $\mathbb{D}_1 = [-0.4, 0.8]^2$. The disturbance and reference are both piece-wise constants, as follows:

$$(d(k), r(k)) = \begin{cases} \left([0, 0.8]^T, [0, 0.5]^T\right), & k \in \mathbb{I}_{0:19} \\ \left([-0.4, -0.4]^T, [-1, 1]^T\right), & k \in \mathbb{I}_{20:39} \\ \left([0.8, 0.8]^T, [-1, 1]^T\right), & k \in \mathbb{I}_{40:60} \end{cases}$$

The weightings are chosen as $Q = R = P_y = P_d = I_2$ and the terminal weighting and terminal controller gain are both calculated from the discrete-time Riccati inequality:

$$P = \begin{bmatrix} 1.96 & 1.17 \\ 1.17 & 2.54 \end{bmatrix}, \ \bar{K} = \begin{bmatrix} -0.74 & -0.80 \\ -0.43 & -0.74 \end{bmatrix}.$$

The prediction horizon N is chosen as 3. The controller and observer gains are chosen as:

$$K = \begin{bmatrix} -0.72 & -0.80 \\ -0.44 & -0.72 \end{bmatrix}, \ L = \begin{bmatrix} 0.5 & -0.5 \\ 0 & 0.5 \end{bmatrix}$$

such that $\rho(A_K) = 0.418$ and $\rho(A_L) = 0.5$. The initial system and observer states are $x(0) = [-2, 1]^T$, $z(0) = [5, -5]^T$.

To realise the proposed APC algorithm, several respective optimisation toolboxes have to be considered. Here, we perform set computation using the MPT3 toolbox (Herceg, Kvasnica, Jones, & Morari, 2013) and solve MPC optimisation using the YALMIP (Lofberg, 2004). The RPI set $\mathbb{S}_K$ is computed by the outer approximation in Rakovic, Kerrigan, Kouramas, and Mayne (2005). The

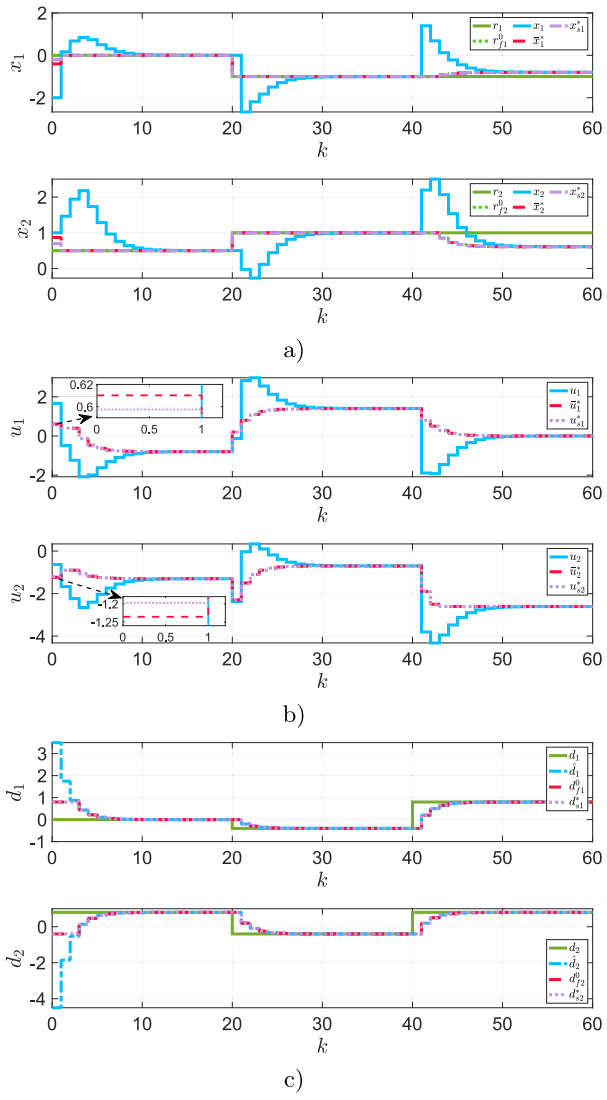

Fig. 7. Trajectories for the numerical example. (a) State-related variables. (b) Input-related variables. (c) Disturbance-related variables.

simulation results are given in Figs. 5–7. Fig. 5(a) and (b) demonstrate the validity of the tightened state and input constraints, which are both non-empty; while Fig. 5(c) presents the calculated steady state and input constraints. Fig. 5(d) geometrically shows the physical meaning of Assumption 7, that is the computed steady state and input constraints are able to provide enough power to survive all the external disturbances. Besides, it is worth noting that the area of the relative complement of $-B_d\mathbb{D}s$ in $(A-I_n)\mathbb{X}_s \oplus B\mathbb{U}_s$ provides a quantification of the system operability, which can be further maximised through parameter optimisation. Fig. 6 shows the evolution of the proposed DEOA set, which varies with the disturbance estimate in the shape. Moreover, Fig. 6 offers geometric interpretations for the optimisation problems $\mathbb{P}_d(\hat{d})$ and $\mathbb{P}_r(d_f^0, r)$, which seek the closest point in $\mathbb{D}_s$ (or $\mathbb{Y}_s$) relative to $\hat{d}$ (or r), respectively. It is worth noting that in the reference governor, the output admissible set is constant and conservative since it should cover all the disturbances in a given set. Fig. 7 shows the convergence of the disturbance estimate to the disturbance and the system IOSD to the optimal steady IOSD. As shown in Figs. 6 and 7, during the periods of $k \in \mathbb{I}_{20:39}$ and $k \in \mathbb{I}_{40:60}$, the given references are hold the same but the external disturbances are changed. Consequently, the tracking

performance is different, i.e., the offset-free tracking can only be achieved during $k \in \mathbb{I}_{20:39}$. This is because when the given reference is out of the DEOA set, the proposed APC will drive the system to the closest position in a safe way. Due to the unknown disturbance, the initial guess on the $\hat{d}(0)$ or $z(0)$ has a large effect on the estimation performance, as shown in Fig. 7(c), which leads large overshoot in the state tracking during the period of $k \in \mathbb{I}_{0:10}$; however, all the states are still kept in the given safe region.

4. Aerial physical interaction

Aerial robotics, i.e., drones, have been widely used in environment monitoring (Coombes, Fletcher, Chen, & Liu, 2020), infrastructure inspection (Jimenez-Cano, Sanchez-Cuevas, Grau, Ollero, & Heredia, 2019) and aerial manipulation tasks (Ollero, Tognon, Suarez, Lee, & Franchi, 2021; Ruggiero, Lippiello, & Ollero, 2018). Their deployment often requires physical interactions with the environment, which in turn poses significant challenges to the safety-critical control design of the drone. The motivating example in Fig. 1 has already revealed the influence of the aerodynamic force, let alone that from the physical contact with the environment. Although pioneers provide solutions at the design level (Rashad et al., 2022; Tognon, Alami, & Siciliano, 2021), the aerial robotics community would still benefit from a unified control framework to deal with those interactions and guarantee safety. In fact, by acknowledging that the disturbance from the environmental contact may not be fully rejected, the proposed APC framework provides an avenue for developing safety-critical control systems operating in unknown environments. This is illustrated in the following case study.[2]

4.1. Control design

The kinematic motion of an aerial robot can be modelled as follows (Beard & McLain, 2012):

$$\begin{aligned} \dot{p} &= Rv \\ \dot{v} &= gR^T n_3 - \frac{T}{m} n_3 + a_d \end{aligned} \tag{25}$$

where $p := [p_x, p_y, p_z]^T \in \mathbb{R}^3$ is the position in the inertial frame; $v := [v_u, v_v, v_w]^T \in \mathbb{R}^3$ is the velocity in the body frame; $R = [c_\theta c_\psi, s_\phi s_\theta c_\psi - c_\phi s_\psi, c_\psi s_\theta c_\phi + s_\psi s_\phi; c_\theta s_\psi, s_\psi s_\theta s_\phi + c_\psi c_\phi, c_\phi s_\theta s_\psi - s_\phi c_\psi; -s_\theta, c_\theta s_\phi, c_\theta c_\phi] \in \mathbb{R}^{3\times 3}$ is the rotation matrix from the body frame to the inertial one and $c_x := \cos(x)$ and $s_x := \sin(x)$, $x \in \{\phi, \theta, \psi\}$; $\phi \in \mathbb{R}$, $\theta \in \mathbb{R}$ and $\psi \in \mathbb{R}$ are the roll, pitch, and yaw angles, respectively; $g \in \mathbb{R}$ is the gravitational acceleration; $m \in \mathbb{R}$ is the mass; $T \in \mathbb{R}$ is the total thrust created by the four propellers; $n_3 := [0, 0, 1]^T \in \mathbb{R}^3$ is the basis vector; $a_d := [a_u, a_v, a_w]^T \in \mathbb{R}^3$ is the acceleration disturbance, which contains the influence from the environment. Here, we use the proposed APC for the positions p_y and p_z and leave the position p_x by using a proportional–integral–derivative (PID) controller. For simplicity, we consider only the outer-loop dynamics of the flight control system and assume that the tracking performance of the inner loop is desirable; the attitude tracking error can be regarded as a disturbance on the outer-loop dynamics. To strictly follow the design approach in this paper, system (25) has to be linearised and discretised first. It is straightforward to obtain the system matrices in the case of zero yaw command, as follows:

$$A = \begin{bmatrix} I_{2\times 2} & t_s I_{2\times 2} \\ 0_{2\times 2} & I_{2\times 2} \end{bmatrix}, B = \begin{bmatrix} 0_{2\times 2} \\ t_s g I_{2\times 2} \end{bmatrix}, B_d = I_4, C = \begin{bmatrix} I_{2\times 2} & 0_{2\times 2} \end{bmatrix}$$

[2] Video available at https://youtube.com/playlist?list=PLpeqs1J7TGl2TBLFEa95V-tHL8rarK8TY.

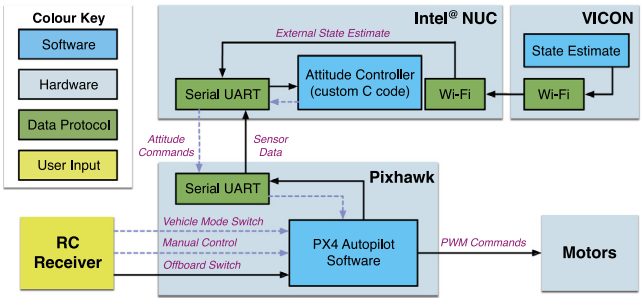

Fig. 8. Configuration of the flight test platform.

where $t_s > 0$ is the sample time in the prediction horizon. The IOSD of drone are denoted by $u(k) = \text{col}(\phi_c(k), 1 - T_c(k)/mg) \in \mathbb{R}^2$, $y(k) = \text{col}(p_y(k), p_z(k)) \in \mathbb{R}^2$, $x(k) = \text{col}(p_y(k), p_z(k), v_v(k), v_w(k)) \in \mathbb{R}^4$ and $d(k) = \text{col}(d_p(k), d_v(k)) \in \mathbb{R}^4$, where $T_c(k)$ and $\phi_c(k)$ are the thrust and roll commands to the inner loop, respectively; $d_p(k) \in \mathbb{R}^2$ and $d_v(k) \in \mathbb{R}^2$ are the disturbances in the position and velocity channels, respectively, which also encompass the modelling error caused by linearisation and backward Euler discretisation, tracking error of the inner loop, and external acceleration disturbance.

The parameters for the drone and controller are given as follows. For the drone, the mass is $m = 1.87$ kg and the gravity is $g = 9.8$ m/s^2. For the observer part, the observer gain is $L = \text{diag}(0.2, 0.2, 0.2, 0.2)$ and the corresponding $\rho(A_L) = 0.8 < 1$. For the controller part, the sample time is $t_s = 1/30$ s, the prediction horizon is $N = 3$, and the weightings are $Q = \text{diag}(1, 1, 10, 10)$, $R = \text{diag}(1, 10)$, $P_d = P_y = 10^3 I_4$. The terminal weighting P and control gain $\bar{K}$ (or K) are computed by the discrete-time Riccati inequality:

$$P = \begin{bmatrix} 969.54 & 0.00 & 50.53 & 0.00 \\ 0.00 & 989.24 & 0.00 & 114.49 \\ 50.53 & 0.00 & 161.62 & 0.00 \\ 0.00 & 114.49 & 0.00 & 373.71 \end{bmatrix}$$

$$\bar{K} = K = \begin{bmatrix} -0.61 & 0.00 & -1.96 & 0.00 \\ 0.00 & -0.27 & 0.00 & -0.88 \end{bmatrix}$$

and the corresponding $\rho(A_{\bar{K}}) = \rho(A_K) = 0.9895 < 1$.

4.2. Experiment results

To implement the proposed APC controller on an onboard computer, we first transfer the constrained optimisation problem (14) into a standard quadratic programming (QP) problem and then use the MATLAB® Coder™ to generate the deployable C code of active-set algorithm for such a QP problem. In the experimental test, we use a Hexsoon 450 quadcopter as a platform. This quadcopter uses a Pixhawk Black 2.1 as a flight controller and a 7th generation Intel i7 NUC to run the proposed control algorithm with the commands generated at 30 Hz. Communication links of the quadcopter are based on the MAVLINK protocol. The configuration of the platform is given by Fig. 8. In the control architecture of PX4 Autopilot, the throttle (within [0,1]) rather than the thrust command is sent to the inner loop. The mapping from the throttle to thrust is nonlinear, and also affected by the battery percentage, but this has been captured in the modelling stage.

As for the quantitative disturbance tests, we use the desk fan and the resistance band as two typical interactions with disturbances. The experimental results are given as follows.

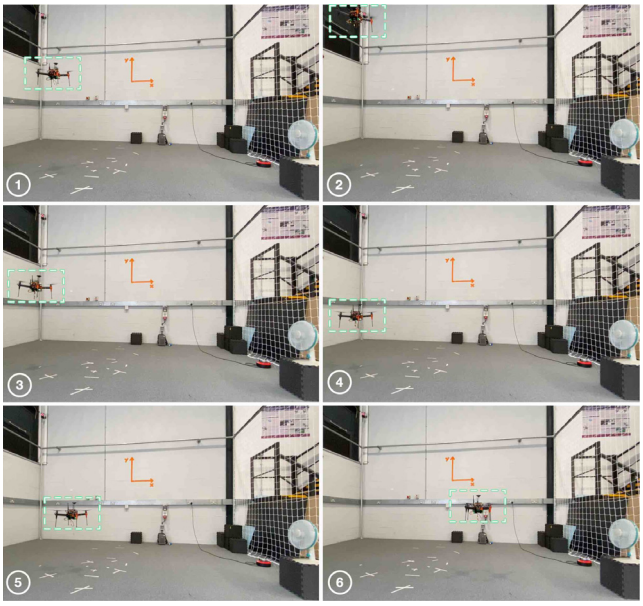

Fig. 9. Snapshots of wind test. ① Ascend; ② Hover at Ref A; ③ Descend; ④ Hover at Ref B; ⑤ Move right; ⑥ Hover at Ref C.

4.2.1. Wind test—Disturbance rejection

A desk fan is used to test the performance of disturbance rejection in a contact-free environment. The desk fan is aligned in the same plane as the reference, whose tests are named as *wind test*. The tests are conducted without the desk fan and at different settings of the fan, representing the cases of no, small, middle and large winds. The pair of reference $(p_{y_r}, -p_{z_r})$ is set as

$$(-1\text{ m}, 2\text{ m}) \underset{\text{Ref A}}{} \xrightarrow[30\text{ s}]{} (-1\text{ m}, 1\text{ m}) \underset{\text{Ref B}}{} \xrightarrow[50\text{ s}]{} (1\text{ m}, 1\text{ m}) \underset{\text{Ref C}}{}$$

which commands the drone to fly towards the desk fan, and hence, the influences from winds are gradually increasing at each test.

The results are given by Figs. 9–11, where the detailed system states and inputs are illustrated in Fig. 11. To show the accuracy improvement, we also compare the proposed method with a simplified version by setting all the disturbance estimates as zeros, which is then in a similar format with Limon et al. (2008, 2010, 2018) and Simon et al. (2014). Although the drone can work in the safe region, large offset tracking errors exist even without any wind disturbances, as shown by the green dotted line in Figs. 10 and 11. This phenomenon can be explained using the analysis of RPI set given in Limon et al. (2010). By contrast, with the appropriate compensation for external disturbance, as shown in Fig. 11(c), the proposed method realises offset-free tracking under different degrees of winds. In other words, these kinds of wind disturbances are fully rejected by the proposed method.

4.2.2. Bungee test—Disturbance coexistence

A resistance band is used to test the performance of disturbance optimal coexistence under the physical environment contact. The resistance band is connected between the drone and anchor on the ground, whose tests are named as *bungee test*. The anchor is located at the origin and the nominal length of the resistance band is $l_c = 1.7$ m. The pair of reference $(p_{y_r}, -p_{z_r})$ is set as

$$(0, 2\text{ m}) \underset{\text{Ref D}}{} \xrightarrow[50\text{ s}]{} (-0.5\text{ m}, 2\text{ m}) \underset{\text{Ref E}}{} \xrightarrow[70\text{ s}]{} (-0.5\text{ m}, 1.5\text{ m}) \underset{\text{Ref F}}{}$$

which commands the drone to fly towards the limit of the resistance band and recover from that limit. It is also worth noting that

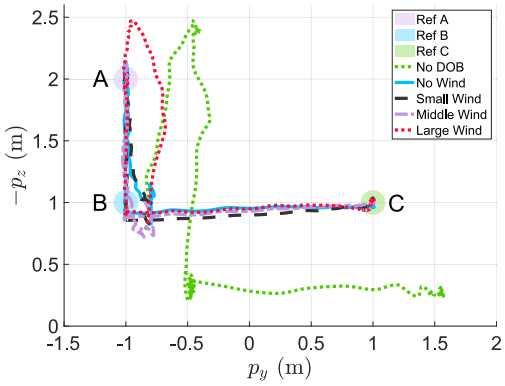

Fig. 10. Tracking performance of wind test in the phase plane. (For interpretation of the references to colour in this figure legend, the reader is referred to the web version of this article.)

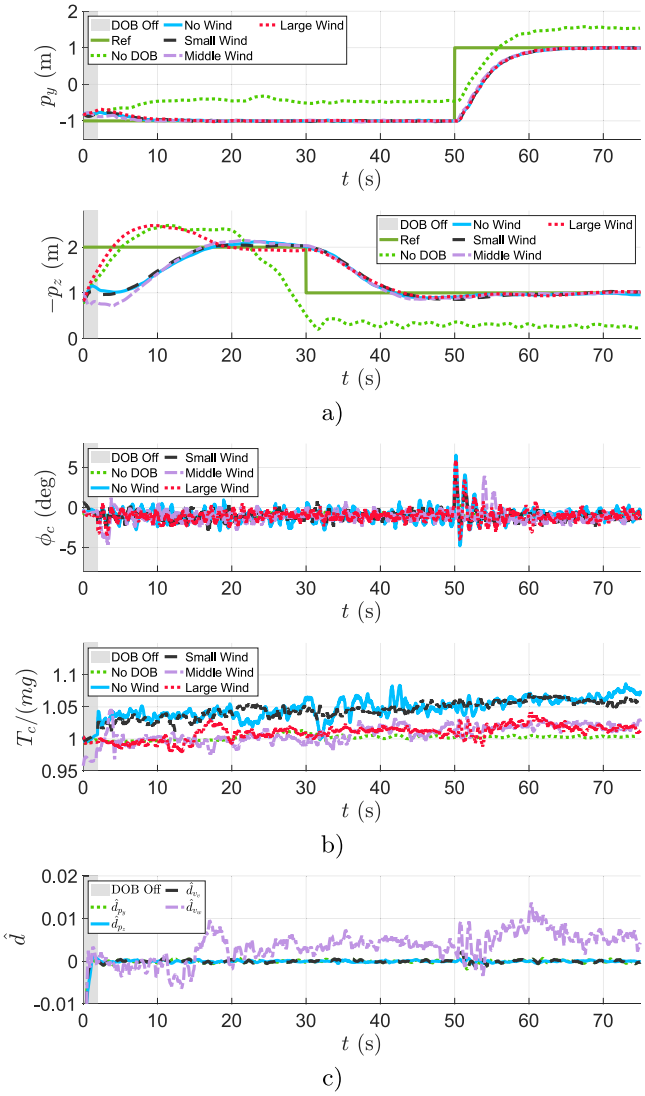

Fig. 11. Wind test. (a) Outputs. (b) Inputs. (c) Disturbance estimates under the large wind. (For interpretation of the references to colour in this figure legend, the reader is referred to the web version of this article.)

the disturbance force from the resistance band is closely related to the drone's position. Following Hooke's law, once the distance between the two ends is longer than the nominal length, the tight

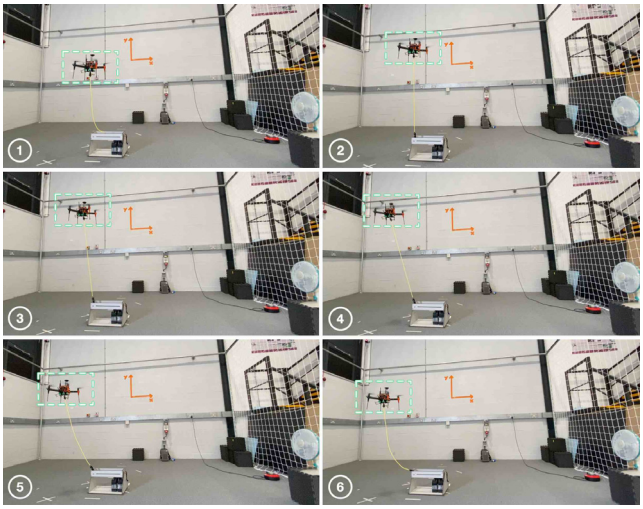

Fig. 12. Snapshots of bungee test. ① Ascend; ② Hover at limit w.r.t. Ref D; ③ Move left; ④ Hover at limit w.r.t. Ref E; ⑤ Descend; ⑥ Hover at Ref F.

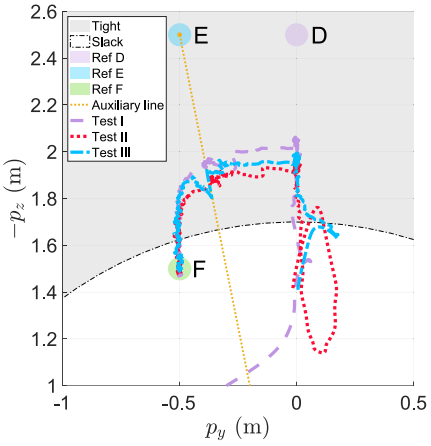

Fig. 13. Tracking performance of bungee test in phase plane.

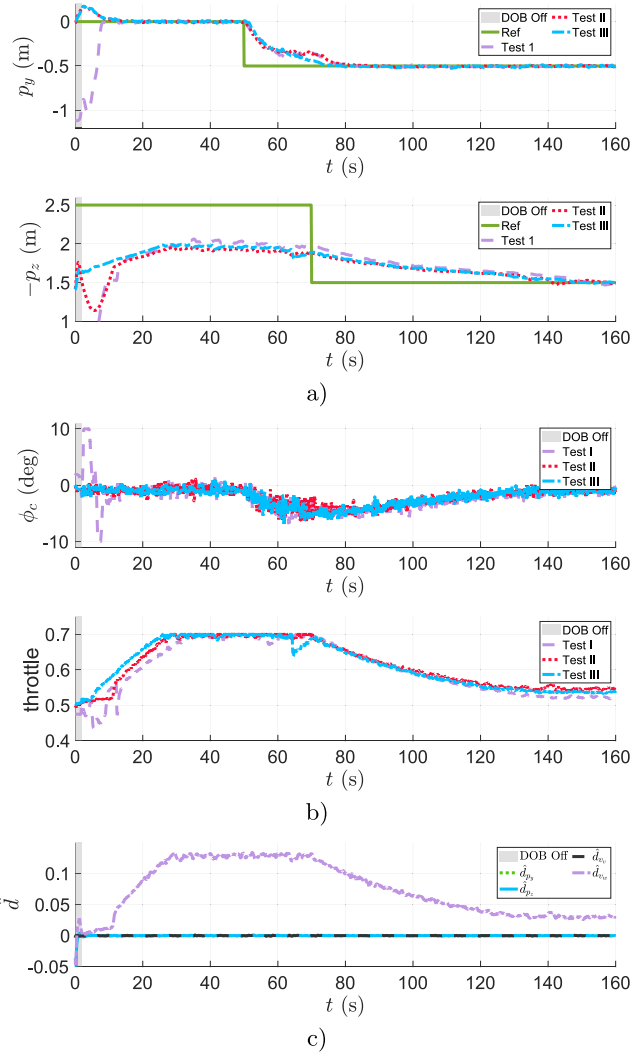

Fig. 14. Bungee test. (a) Outputs. (b) Inputs. (c) Disturbance estimates of Test I.

resistance band would generate internal force $F_c = k_c(|p| - l_c)$, where k_c is the elastic coefficient; and if the distance is not longer than the nominal length, the resistance band would be slack and generate zero internal force.

To show the consistency of the proposed controller, the bungee tests are repeated three times, where the first test started slightly left of the anchor and the rest two tests started directly above the anchor. The results are given by Figs. 12–14. In Fig. 13, Refs D and E are obvious in the tight region of the resistance band and are quite difficult to be tracked. All these tests show that the proposed controller drives the drone to the optimal positions in the sense that the drone statically stays in the best direction between the unreachable references and the origin, as shown in Fig. 13 and the throttle commands reach the given maximum 70%, as shown in Fig. 14(b). In Fig. 13, although the limit w.r.t Ref E or D at each test is slightly different (mainly due to the decreasing battery percentages), the drone can always find this optimal point and stay in it by using the real-time disturbance estimates. Generally, the disturbances when the drone is tried to track Refs D and E are unable to be fully rejected due to the physical limitations and these three tests all show that the proposed method can make the drone optimally coexist with such disturbances. As for the Ref F, offset-free tracking can be achieved as shown in Figs. 13 and 14(a). It is also interesting to note that the disturbance estimates at the end of the bungee test are higher than that in the wind test, which is mainly caused by the weight of the resistance band itself.

4.2.3. Computation resource

Real-time computation is critical for the proposed method, not only because the constrained optimisation-based control, $\mathbb{P}_N(x, d_f^0, r_f^0)$, needs to be solved online, but also due to the monitor mechanism to choose disturbance rejection or coexistence, $\mathbb{P}_d(\hat{d})$ and $\mathbb{P}_r(d_f^0, r)$. Fortunately, with the linear formulation, all the optimisation modules can be straightforwardly rewritten as QP problems and multiple well-developed toolkits are available. The computation time of each optimisation module by using the default QP of Matlab is given by Fig. 15, where the observer module contains the DOB itself (4) and the optimisation problem $\mathbb{P}_d(\hat{d})$ in (7); the reference module contains the optimisation problem $\mathbb{P}_r(d_f^0, r)$ in (10); the controller module contains the explicit controller (12) and the optimisation problem $\mathbb{P}_N(x, d_f^0, r_f^0)$ in (14). It is worth noting that the observer module takes the least computation time, which has to be enlarged 100 times for clear visualisation. The total computation time of all these three modules is given by the grey columns in Fig. 15, which is much smaller than the sample time $t_s = 33.33$ ms and proves the real-time computation property of the proposed method.

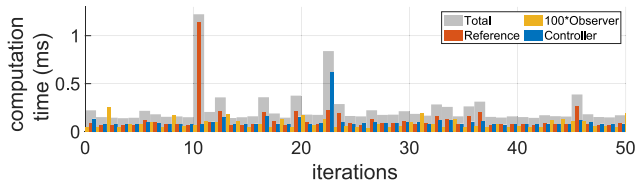

Fig. 15. Computation time of each optimisation module.

5. Conclusions

In this paper, we have built a unified framework to achieve safety-critical control for dynamic systems under disturbances. Different from most existing tracking designs, the proposed framework has provided an alternative but safer way, starting from surviving all disturbances but taking every opportunity to reject them. To realise this goal, a new optimisation-based controller with an augmented setup has been proposed, not only in the additional penalties on the disturbance rejection and output tracking in the modified cost function but also in the pseudo steady disturbance-driven prediction model. Moreover, this more flexible setup has been proven to guarantee the recursive feasibility of constrained dynamic optimisation and offset-free tracking to an optimal reachable target. Numerical simulation and aerial physical interaction tests have been both carried out to show the features and effectiveness of the proposed method. Future work will focus on optimising design parameters to maximise operability.

Acknowledgements

This work was supported in part by the UK Engineering and Physical Sciences Research Council (EPSRC) Established Career Fellowship "Goal-oriented control systems: Disturbance, uncertainty and constraints" under the Grant Number EP/T005734/1, in part by UK EPSRC First Grant "Autonomous landing of a helicopter at sea: Advanced control in adverse conditions" under the Grant Number EP/P012868/1. Dr. Y. Yan would like to express his heartfelt thanks to all the members of the Loughborough University Centre for Autonomous Systems (LUCAS) who have offered their altruistic help in this paper.

Appendix

The appendix collects the detailed proofs on recursive feasibility and stability, and the verification of Assumption 11. On the proof of recursive feasible, although it looks like to follow the standard way in the conventional MPC literature, the explicit embedding of a pseudo steady disturbance $d_s(k)$ as a decision variable makes it possible to keep the prediction model unchangeable, even when the disturbance or its estimate changes rapidly. This means that such a design way is the key point to guarantee recursive feasibility, which cannot be strictly satisfied in the conventional offset-free MPC as the disturbance estimate is directly involved in its prediction model. Furthermore, to guarantee the stability of the proposed robust tracking MPC framework, a novel non-quadratic Lyapunov function consists of the value function from APC and the disturbance estimation error is constructed, which is different from Lyapunov construction of the conventional MPC. In addition, a contradiction method is used to prove that the optimal pseudo steady output and disturbance can converge to the desirable ones.

Appendix A. Proof of Theorem 16

Proof. The optimal nominal state and control at time k are denoted by:

$$\bar{\mathbf{u}}^*(k) := \left(\bar{u}^*(0;k), \bar{u}^*(1;k), \dots, \bar{u}^*(N-1;k)\right)$$
$$\bar{\mathbf{x}}^*(k) := \left(\bar{x}^*(0;k), \bar{x}^*(1;k), \dots, \bar{x}^*(N-1;k), \bar{x}^*(N;k)\right)$$

and the optimal steady IOSD are $u_s^*(k)$, $y_s^*(k)$, $x_s^*(k)$, and $d_s^*(k)$.

We first construct the following sequences (A.1), which will be proved to be feasible at time $k+1$:

$$\begin{aligned}
\bar{\mathbf{u}}(k+1) :=& \Big(\bar{u}^*(1;k), \dots, \bar{u}^*(N-1;k), \\
& \qquad \bar{K}(\bar{x}^*(N;k) - x_s^*(k)) + u_s^*(k) \Big) \\
\bar{\mathbf{x}}(k+1) :=& \Big(\bar{x}^*(1;k), \dots, \bar{x}^*(N-1;k), \bar{x}^*(N;k), \\
& \qquad A_{\bar{K}}(\bar{x}^*(N;k) - x_s^*(k)) + x_s^*(k) \Big) \\
x_s(k+1) :=& x_s^*(k), \;\; u_s(k+1) := u_s^*(k) \\
y_s(k+1) :=& y_s^*(k), \;\; d_s(k+1) := d_s^*(k).
\end{aligned} \tag{A.1}$$

In (A.1), constraint (14a) holds for time $k+1$ due to the positive invariance of $\mathbb{S}_K$. By choosing $d_s(k+1) = d_s^*(k)$, the nominal model (14b) is the same with that at time k. Hence, the last $N-1$ terms of the optimal state/input trajectory at time k, i.e., $\bar{\mathbf{x}}^*(k)$ and $\bar{\mathbf{u}}^*(k)$, are admissible at time $k+1$, and hence, are used to construct the feasible sequence (A.1), which implies constraints (14b) and (14c) both hold for time $k+1$. Constraint (14d) holds due to the positive invariance of $\Theta_{\bar{K}}$. Constraints (14e) and (14f) hold since the feasible steady IOSD at time $k+1$ are chosen the same as the optimal ones at time k. Hence, the sequence (A.1) is feasible for time $k+1$, which completes the proof. ■

Appendix B. Proof of Theorem 18

Before presenting the proof of Theorem 18, we will first give one lemma to reveal the relationships among the optimal IOSD.

Lemma 20. *Suppose that the optimal solutions of $\mathbb{P}_N(x, d_f^0, r_f^0)$ in (14) satisfy $\bar{x}^*(0;k) = x_s^*(k)$ and $\bar{u}^*(0;k) = u_s^*(k)$. Then, the rest of the optimal solutions are $d_s^*(k) = d_f^0(k)$ and $y_s^*(k) = r_f^0(k)$ and the value function $V_N^*(\bar{x}^*(0;k) - x_s^*(k), d_f^0(k) - d_s^*(k), r_f^0(k) - y_s^*(k)) = 0$.*

Proof. It will be proved by contradiction. Assume that $\bar{x}^*(0;k) = x_s^*(k)$ and $\bar{u}^*(0;k) = u_s^*(k)$, but $y_s^*(k) \neq y_s^0(k)$ or $d_s^*(k) \neq d_s^0(k)$. Recalling the conclusion of $d_f^0(k) = d_s^0(k)$ and $r_f^0(k) = y_s^0(k)$ in Lemma 13, we will have $V_N^*(k) = V_d(d_s^0(k) - d_s^*(k)) + V_y(y_s^0(k) - y_s^*(k)) > 0$, where $V_N^*(\bar{x}^*(0;k) - x_s^*(k), d_f^0(k) - d_s^*(k), r_f^0(k) - y_s^*(k))$ is denoted as $V_N^*(k)$ for the notation simplification.

Consider a perturbation of $x_s^*(k)$ towards $x_s^0(k)$, given by:

$$\tilde{x}_s(k) := \gamma x_s^*(k) + (1-\gamma) x_s^0(k), \;\; \gamma \in [0,1]. \tag{B.1}$$

Similarly, $\tilde{u}_s(k)$, $\tilde{d}_s(k)$ and $\tilde{y}_s(k)$ can be defined in this way. Due to the convexity, we have $\tilde{x}_s(k) \in \mathbb{X}_s$, $\tilde{u}_s(k) \in \mathbb{U}_s$, and $\tilde{d}_s(k) \in \mathbb{D}_s$. It is quite straightforward to have that the quartet $(\tilde{u}_s(k), \tilde{y}_s(k), \tilde{x}_s(k), \tilde{d}_s(k))$ is also the steady IOSD, i.e., $\tilde{x}_s(k) = A\tilde{x}_s(k) + B\tilde{u}_s(k) + B_d\tilde{d}_s(k)$. Next, starting at $\bar{x}(0;k) = x_s^*(k)$ and applying a constant input $\bar{u}(i;k) = \tilde{u}_s(k)$, $i \in \mathbb{I}_{1:N-1}$ will obtain the following predicted states:

$$\bar{x}(i;k) = (1-\gamma) A^i \left(x_s^*(k) - x_s^0(k)\right) + \tilde{x}_s(k) \tag{B.2}$$

where $i \in \mathbb{I}_{0:N}$. Then, we can construct the following sequences (B.3):

$$\begin{aligned}
&\bar{\mathbf{u}}(k) := \left(\tilde{u}_s(k), \ldots, \tilde{u}_s(k)\right)\\
&\bar{\mathbf{x}}(k) := \left(x_s^*(k), \ldots, (1-\gamma)A^N\left(x_s^*(k) - x_s^0(k)\right) + \tilde{x}_s(k)\right)\\
&x_s(k) := \tilde{x}_s(k),\ u_s(k) := \tilde{u}_s(k)\\
&y_s(k) := \tilde{y}_s(k),\ d_s(k) := \tilde{d}_s(k).
\end{aligned} \tag{B.3}$$

With the similar analysis in Alvarado (2007, Proof of Lemma 3.2), the sequences in (B.3) are feasible if γ is sufficiently close to 1. The stage, terminal, disturbance rejection and output tracking costs can be easily computed as follows:

$$\begin{aligned}
&\ell\left(\bar{x}(i;k) - x_s(k), \bar{u}(i;k) - u_s(k)\right) = (1-\gamma)^2\left|x_s^*(k) - x_s^0(k)\right|^2_{A^{iT}QA^i}\\
&V_f(\bar{x}(N;k) - x_s(k)) = (1-\gamma)^2\left|x_s^*(k) - x_s^0(k)\right|^2_{A^{NT}PA^N}\\
&V_d\left(d_f^0(k) - d_s(k)\right) = \gamma^2\left|d_s^*(k) - d_s^0(k)\right|^2_{P_d}\\
&V_y\left(r_f^0(k) - y_s(k)\right) = \gamma^2\left|y_s^*(k) - y_s^0(k)\right|^2_{P_y}
\end{aligned}$$

and the total cost is given by:

$$\begin{aligned}
V_N(k) = (1-\gamma)^2&\left|x_s^*(k) - x_s^0(k)\right|^2_{\Psi_N}\\
&+ \gamma^2\left|d_s^*(k) - d_s^0(k)\right|^2_{P_d} + \gamma^2\left|y_s^*(k) - y_s^0(k)\right|^2_{P_y}
\end{aligned} \tag{B.4}$$

where $\Psi_N := \sum_{i=0}^{N-1} A^{iT}QA^i + A^{NT}QA^N$. Taking the differential $V_N(k)$ in (B.4) with respect to the γ and evaluating it at $\gamma = 1$ gives that:

$$\left.\frac{\partial V_N(k)}{\partial \gamma}\right|_{\gamma=1} = 2\left(\left|d_s^*(k) - d_s^0(k)\right|^2_{P_d} + \left|y_s^*(k) - y_s^0(k)\right|^2_{P_y}\right) > 0 \tag{B.5}$$

which implies that by decreasing γ from 1 to any value sufficiently close to 1, $V_N(k)$ can be decreased. It will cause a contradiction with the fact of $V_N^*(k) = V_N(k)|_{\gamma=1}$. Hence, we have $d_s^*(k) = d_f^0(k)$ and $y_s^*(k) = r_f^0(k)$.

By choosing $\bar{u}(i;k) = u_s(k)$, $i \in \mathbb{I}_{1:N-1}$, which leads $\bar{x}(i;k) = x_s(k)$, $i \in \mathbb{I}_{1:N}$, we obtain $V_N^*(k) = V_d(d_f^0(k) - d_s^*(k)) + V_y(y_s^0(k) - y_s^*(k)) = 0$. Thus, the conclusions of Lemma 20 follow. ■

To make the reader easily understand the proof of Theorem 18, we will first prove the first part (points (i) and (ii)), then the second part (points (iii) and (iv)).

Proof of the first part of Theorem 18. Due to the recursive feasibility, the safety of the closed-loop system can be guaranteed. Hence, in the theoretical analysis of the stability, we only need to consider the time $k \geq k_1$, i.e., $\tilde{d}(k)$ will be captured by $\mathbb{D}_L$. Then, $d_f^0(k) = \hat{d}(k)$ holds for all $k \geq k_1$. If the disturbance is a constant at the steady state, the proposed DOB is asymptotically stable, i.e., $\lim_{k\to\infty}\tilde{d}(k) = 0$, then $\lim_{k\to\infty} d_f^0(k) = d_c$.

To clearly show the proof of the first part, we divide the proof of this part into the following two steps:

(1) *Step One:* Prove the convergence of the nominal state and input to the optimal pseudo steady ones;
(2) *Step Two:* Prove the convergence of the optimal pseudo steady output and disturbance to the target ones.

Step One:

Using the standard procedures in MPC proof, we first compare the value function of $\mathbb{P}_N(x, d_f^0, r_f^0)$ at time k with the cost under the feasible sequences (A.1) at time $k+1$. The value function at time k is given by:

$$\begin{aligned}
&V_N^*(k)\\
&= \sum_{i=0}^{N-1}\ell\left(\bar{x}^*(i;k) - x_s^*(k), \bar{u}^*(i;k) - u_s^*(k)\right)\\
&\quad + V_f\left(\bar{x}^*(N;k) - x_s^*(k)\right)\\
&\quad + V_d\left(d_f^0(k) - d_s^*(k)\right) + V_y\left(r_f^0(k) - y_s^*(k)\right)
\end{aligned} \tag{B.6}$$

and the cost function under the feasible sequences (A.1) at time $k+1$ is given by:

$$\begin{aligned}
&V_N(k+1)\\
&= \sum_{i=1}^{N-1}\ell\left(\bar{x}^*(i;k) - x_s^*(k), \bar{u}^*(i;k) - u_s^*(k)\right)\\
&\quad + \ell\left(\bar{x}^*(N;k) - x_s^*(k), \bar{K}\left(\bar{x}^*(N;k) - x_s^*(k)\right)\right)\\
&\quad + V_f\left(A_{\bar{K}}\left(\bar{x}^*(N;k) - x_s^*(k)\right)\right)\\
&\quad + V_d\left(d_f^0(k+1) - d_s^*(k)\right)\\
&\quad + V_y\left(r_f^0(k+1) - y_s^*(k)\right).
\end{aligned} \tag{B.7}$$

To clearly compare $V_N^*(k)$ with $V_N(k+1)$, the differences in the disturbance rejection cost $V_d(\cdot)$ and output tracking cost $V_y(\cdot)$ need to be computed first. It follows from (5) that:

$$\begin{aligned}
&V_d\left(d_f^0(k+1) - d_s^*(k)\right) - V_d\left(d_f^0(k) - d_s^*(k)\right)\\
&\leq c_1\left|\left(d_f^0(k+1) - d_s^*(k)\right) - \left(d_f^0(k) - d_s^*(k)\right)\right|\\
&= c_1\left|d_f^0(k+1) - d_f^0(k)\right| = c_1\left|\hat{d}(k+1) - \hat{d}(k)\right|\\
&= c_1\left|(A_L - I_{n_d})\tilde{d}(k)\right|
\end{aligned} \tag{B.8}$$

and by Assumption 11, similarly, we have:

$$\begin{aligned}
&V_y\left(r_f^0(k+1) - y_s^*(k)\right) - V_y\left(r_f^0(k) - y_s^*(k)\right)\\
&\leq c_2\left|r_f^0(k+1) - r_f^0(k)\right| \leq c_2 c_r\left|\hat{d}(k+1) - \hat{d}(k)\right|
\end{aligned} \tag{B.9}$$

for some Lipschitz constants $c_1, c_2 > 0$. Subtracting (B.6) from (B.7) and keeping (23), (B.8) and (B.9) in mind gives that:

$$\begin{aligned}
&V_N^*(k+1) - V_N^*(k) \leq V_N(k+1) - V_N^*(k)\\
&\leq -\left|\bar{x}^*(0;k) - x_s^*(k)\right|^2_Q - \left|\bar{u}^*(0;k) - u_s^*(k)\right|^2_R + c\left|\tilde{d}(k)\right|
\end{aligned} \tag{B.10}$$

where $c := (c_1 + c_2 c_r)|A_L - I_{n_d}| > 0$.

Define $W(k) := V_N^*(k) + \mu|\tilde{d}(k)|$, where $\mu := c/(1 - |A_L|) > 0$. Using (5) and (B.10), we obtain:

$$\begin{aligned}
&W(k+1) - W(k)\\
&\leq \mu(|A_L| - 1)\left|\tilde{d}(k)\right| + c\left|\tilde{d}(k)\right|\\
&\quad - \left|\bar{x}^*(0;k) - x_s^*(k)\right|^2_Q - \left|\bar{u}^*(0;k) - u_s^*(k)\right|^2_R\\
&\leq -\left|\bar{x}^*(0;k) - x_s^*(k)\right|^2_Q - \left|\bar{u}^*(0;k) - u_s^*(k)\right|^2_R,
\end{aligned} \tag{B.11}$$

which implies that $W(k)$ is non-increasing. Noting $W(k) \geq 0$ and using the monotone convergence theorem, we have that the limit of $W(k)$ exists, denoted as $W(\infty) := \lim_{k\to\infty} W(k)$. The existence of $W(\infty)$ implies that the items on the right-hand side of (B.11) converge to zero, that is

$$\begin{aligned}
&\lim_{k\to\infty}\bar{x}^*(0;k) - x_s^*(k) = 0,\ \lim_{k\to\infty}\bar{u}^*(0;k) - u_s^*(k) = 0\\
&\Rightarrow \lim_{k\to\infty}\bar{y}^*(0;k) - y_s^*(k) = 0.
\end{aligned} \tag{B.12}$$

Step Two:

In what follows, we will prove that once the nominal state/input goes to the optimal steady state/input, the nominal output will go to the target output.

From Lemma 20, we know that if $\bar{x}^*(0;k) = x_s^*(k)$ and $\bar{u}^*(0;k) = u_s^*(k)$, $V_N^*(k) = 0$ holds. Noting that $W(k) = W(\bar{x}^*(0;k) - x_s^*(k), d_f^0(k) - d_s^*(k), r_f^0(k) - y_s^*(k), \tilde{d}(k))$ is continuous with respect to each element and its limit exists, we have:

$$W(\infty) = \lim_{k\to\infty} W\Big(\lim_{k\to\infty} \bar{x}^*(0;k) - x_s^*(k), d_f^0(k) - d_s^*(k), r_f^0(k) - y_s^*(k), \lim_{k\to\infty} \tilde{d}(k)\Big) = \lim_{k\to\infty} V_N^*\left(0, d_f^0(k) - d_s^*(k), r_f^0(k) - y_s^*(k)\right) = 0,$$

which implies that:

$$\lim_{k\to\infty} \bar{y}^*(0;k) = \lim_{k\to\infty} y_s^*(k) = \lim_{k\to\infty} y_s^0(k) = r_{fc}^0$$
$$\lim_{k\to\infty} d_s^*(k) = \lim_{k\to\infty} d_s^0(k) = \lim_{k\to\infty} d_f^0(k) = d_c. \tag{B.13}$$

Thus, from the invariance of the tube $\mathbb{S}_K$, we can conclude that the real output will tend to $\{r_{fc}^0\} \oplus C\mathbb{S}_K$, which completes the proof. ■

Proof of the second part of Theorem 18. By Assumption 17, we have that the limits of $x_s^0(k)$ and $u_s^0(k)$ exist:

$$\begin{bmatrix} x_s^0(\infty) \\ u_s^0(\infty) \end{bmatrix} := \begin{bmatrix} \lim_{k\to\infty} x_s^0(k) \\ \lim_{k\to\infty} u_s^0(k) \end{bmatrix} = \begin{bmatrix} A - I_n & B \\ C & 0_{p\times m} \end{bmatrix}^{-1} \begin{bmatrix} -B_d d_c \\ r_{fc}^0 \end{bmatrix}. \tag{B.14}$$

From (B.13), we have that the limits of $x_s^*(k)$ and $u_s^*(k)$ exist and are the same with (B.14), as follows:

$$\begin{bmatrix} x_s^*(\infty) \\ u_s^*(\infty) \end{bmatrix} := \begin{bmatrix} \lim_{k\to\infty} x_s^*(k) \\ \lim_{k\to\infty} u_s^*(k) \end{bmatrix} = \begin{bmatrix} x_s^0(\infty) \\ u_s^0(\infty) \end{bmatrix}. \tag{B.15}$$

Taking the controller (12) into system (1) gives:

$$e_x(k+1) = A_K e_x(k) + w(k) \tag{B.16}$$

where $e_x(k) := x(k) - x_s^*(k)$ and $w(k) := -(x_s^*(k+1) - x_s^*(k)) + B(\bar{u}^*(0;k) - u_s^*(k)) + B_d(d(k) - d_s^*(k))$. According to the previous analysis of (B.12) and (B.13), $w(k)$ will go to zero as time goes to the infinity. Applying the property of ISS yields:

$$\lim_{k\to\infty} e_x(k) = 0 \Rightarrow \lim_{k\to\infty} x(k) = x_s^*(\infty) \tag{B.17}$$

and then we obtain:

$$\lim_{k\to\infty} y(k) = \lim_{k\to\infty} Cx(k) = r_{fc}^0, \tag{B.18}$$

which completes the proof. ■

Appendix C. Verification of Assumption 11

Transforming the optimisation problem (10) $\mathbb{P}_r(d_f^0, r)$ into a multi-parametric quadratic program (mp-QP) problem depends on the solution sets of $\mathtt{A}\mathtt{x} = \mathtt{b}$, where $\mathtt{A} := [A - I_n, B]$, $\mathtt{x} := \mathrm{col}(x_s, u_s)$, and $\mathtt{b} := -B_d d_s$. Hence, a systematic analysis would make the process unnecessarily complicated. As a result, we have chosen to focus solely on two examples in this paper for the sake of clarity and simplicity.

The following definition on the piecewise affine function (Bemporad et al., 2002, Defin. 1) and the fundamental theorem on the solution of mp-QP (Bemporad et al., 2002, Thm. 4) are used in the verification of Assumption 11.

Definition 21. A function $z(x) : \mathbb{X} \mapsto \mathbb{R}^s$, where $\mathbb{X} \subseteq \mathbb{R}^n$ is a polyhedral set, is piecewise affine if it is possible to partition $\mathbb{X}$ into convex polyhedral regions, CR_i, $i \in \mathbb{I}_{\geq 1}$, and $z(x) = H^i x + k^i$, $\forall x \in CR_i$.

Lemma 22. *Consider the following mp-QP:*

$$z^0(x) := \arg\min_z \frac{1}{2} z^T H z \quad \text{s.t. } Gz \leq W + Sx \tag{C.1}$$

and let $H > 0$ and $\mathbb{X}$ convex, where $\mathbb{X}$ is the set of feasible parameters. Then the optimiser $z^0(x) : \mathbb{X} \mapsto \mathbb{R}^s$ is continuous and piecewise affine.

We assume that $\mathbb{X}_s$, $\mathbb{U}_s$ and $\mathbb{D}_s$ can be represented by polyhedral sets, i.e.,

$$\mathbb{X}_s := \{x_s \in \mathbb{R}^n \mid A_x x_s \leq b_x\}$$
$$\mathbb{U}_s := \{u_s \in \mathbb{R}^m \mid A_u u_s \leq b_u\}$$
$$\mathbb{D}_s := \{d_s \in \mathbb{R}^{n_d} \mid A_d d_s \leq b_d\}.$$

C.1. Numerical Example in Section 3.7

In this example, noting that $A - I_2$ is invertable, $y_s = -C(A - I_2)^{-1}(Bu_s + B_d d_s)$. Hence, the optimisation problem (10) can be transformed as follows:

$$u_s^0(d_f^0) := \arg\min_{u_s} \left| -C(A - I_2)^{-1}(Bu_s + B_d d_f^0) - r \right|^2$$
$$\text{s.t. } A_u u_s \leq b_u,$$
$$-A_x(A - I_2)^{-1}(Bu_s + B_d d_f^0) \leq b_x$$

and $r_f^0(d_f^0) = -C(A-I_2)^{-1}(Bu_s^0(d_f^0)+B_d d_f^0)$. By completing squares, we can obtain the standard format in (C.1) where $H = 2(C(A - I_2)^{-1}B)^T(C(A - I_2)^{-1}B) > 0$. The fact that $r_f^0(d_f^0)$ is continuous and piecewise affine, follows trivially.

C.2. Physical Example in Section 4

In this example, $[A - I_4, B] = [0_{4\times 2}, \mathrm{diag}(t_s, t_s, t_s g, t_s g)]$, which implies $x_{s,3}, x_{s,4}, u_{s,1}, u_{s,2}$ can all be constructed by $x_{s,1}, x_{s,2}$. Hence, the optimisation problem (10) can be transformed into an mp-QP with 2-dimensional decision variables. The same fact on $H > 0$ and $r_f^0(d_f^0)$, follows trivially.

References

Alvarado, I. (2007). *Model predictive control for tracking constrained linear systems* (Ph.D. thesis), Department of Systems Engineering and Automation, University of Sevilla.

Ames, A. D., Coogan, S., Egerstedt, M., Notomista, G., Sreenath, K., & Tabuada, P. (2019). Control barrier functions: Theory and applications. In *European control conference* (pp. 3420–3431).

Ames, A. D., Xu, X., Grizzle, J. W., & Tabuada, P. (2016). Control barrier function based quadratic programs for safety critical systems. *IEEE Transactions on Automatic Control*, *62*(8), 3861–3876.

Beard, R. W., & McLain, T. W. (2012). *Small unmanned aircraft: Theory and practice*. Princeton University Press.

Bemporad, A., Morari, M., Dua, V., & Pistikopoulos, E. N. (2002). The explicit linear quadratic regulator for constrained systems. *Automatica*, *38*(1), 3–20.

Betti, G., Farina, M., & Scattolini, R. (2013). A robust MPC algorithm for offset-free tracking of constant reference signals. *IEEE Transactions on Automatic Control*, *58*(9), 2394–2400.

Boyd, S., Boyd, S. P., & Vandenberghe, L. (2004). *Convex optimization*. Cambridge University Press.

Bratta, A., Focchi, M., Rathod, N., Zanon, M., Bemporad, A., & Semini, C. (2022). Governor: A reference generator for nonlinear model predictive control in legged robots. arXiv preprint arXiv:2207.10175.

Carron, A., Arcari, E., Wermelinger, M., Hewing, L., Hutter, M., & Zeilinger, M. N. (2019). Data-driven model predictive control for trajectory tracking with a robotic arm. *IEEE Robotics and Automation Letters*, *4*(4), 3758–3765.

Chen, W.-H., Ballance, D. J., Gawthrop, P. J., & O'Reilly, J. (2000). A nonlinear disturbance observer for robotic manipulators. *IEEE Transactions on Industrial Electronics*, *47*(4), 932–938.

Chen, W.-H., Yang, J., Guo, L., & Li, S. (2015). Disturbance-observer-based control and related methods—An overview. *IEEE Transactions on Industrial Electronics*, *63*(2), 1083–1095.

Chisci, L., Rossiter, J. A., & Zappa, G. (2001). Systems with persistent disturbances: Predictive control with restricted constraints. *Automatica*, *37*(7), 1019–1028.

Coombes, M., Fletcher, T., Chen, W.-H., & Liu, C. (2020). Decomposition-based mission planning for fixed-wing UAVs surveying in wind. *Journal of Field Robotics*, *37*(3), 440–465.

Corsini, G., Jacquet, M., Das, H., Afifi, A., Sidobre, D., & Franchi, A. (2022). Nonlinear model predictive control for human-robot handover with application to the aerial case. In *IEEE/RSJ international conference on intelligent robots and systems*.

Daş, E., & Murray, R. M. (2022). Robust safe control synthesis with disturbance observer-based control barrier functions. In *IEEE conference on decision and control* (pp. 5566–5573).

El Yaagoubi, E., El Assoudi, A., & Hammouri, H. (2004). High gain observer: Attenuation of the peak phenomena. In *American control conference, Vol. 5* (pp. 4393–4397).

Farzan, S., Azimi, V., Hu, A.-P., & Rogers, J. (2022). Adaptive control of wire-borne underactuated brachiating robots using control Lyapunov and barrier functions. *IEEE Transactions on Control Systems Technology*, *30*(6), 2598–2614.

Ferraguti, F., Landi, C. T., Singletary, A., Lin, H.-C., Ames, A., Secchi, C., et al. (2022). Safety and efficiency in robotics: The control barrier functions approach. *IEEE Robotics & Automation Magazine*, *29*(3), 139–151.

Garone, E., Di Cairano, S., & Kolmanovsky, I. (2017). Reference and command governors for systems with constraints: A survey on theory and applications. *Automatica*, *75*, 306–328.

Gilbert, E. G., & Tan, K. T. (1991). Linear systems with state and control constraints: The theory and application of maximal output admissible sets. *IEEE Transactions on Automatic Control*, *36*(9), 1008–1020.

Herceg, M., Kvasnica, M., Jones, C., & Morari, M. (2013). Multi-parametric toolbox 3.0. In *Proceedings of the european control conference* (pp. 502–510).

Hewing, L., Wabersich, K. P., Menner, M., & Zeilinger, M. N. (2020). Learning-based model predictive control: Toward safe learning in control. *Annual Review of Control, Robotics, and Autonomous Systems*, *3*, 269–296.

Huang, Y., Hofer, M., & D'Andrea, R. (2021). Offset-free model predictive control: A ball catching application with a spherical soft robotic arm. In *IEEE/RSJ international conference on intelligent robots and systems* (pp. 563–570).

Incremona, G. P., Ferrara, A., & Magni, L. (2017). MPC for robot manipulators with integral sliding modes generation. *IEEE/ASME Transactions on Mechatronics*, *22*(3), 1299–1307.

Isidori, A. (1995). *Nonlinear control systems* (3rd ed.). Springer.

Jiang, Z.-P., & Wang, Y. (2001). Input-to-state stability for discrete-time nonlinear systems. *Automatica*, *37*(6), 857–869.

Jimenez-Cano, A. E., Sanchez-Cuevas, P. J., Grau, P., Ollero, A., & Heredia, G. (2019). Contact-based bridge inspection multirotors: Design, modeling, and control considering the ceiling effect. *IEEE Robotics and Automation Letters*, *4*(4), 3561–3568.

Kolmanovsky, I., Garone, E., & Di Cairano, S. (2014). Reference and command governors: A tutorial on their theory and automotive applications. In *American control conference* (pp. 226–241).

Limon, D., Alvarado, I., Alamo, T., & Camacho, E. F. (2008). MPC for tracking piecewise constant references for constrained linear systems. *Automatica*, *44*(9), 2382–2387.

Limon, D., Alvarado, I., Alamo, T., & Camacho, E. F. (2010). Robust tube-based MPC for tracking of constrained linear systems with additive disturbances. *Journal of Process Control*, *20*(3), 248–260.

Limon, D., Ferramosca, A., Alvarado, I., & Alamo, T. (2018). Nonlinear MPC for tracking piece-wise constant reference signals. *IEEE Transactions on Automatic Control*, *63*(11), 3735–3750.

Lindqvist, B., Mansouri, S. S., Agha-mohammadi, A.-a., & Nikolakopoulos, G. (2020). Nonlinear MPC for collision avoidance and control of UAVs with dynamic obstacles. *IEEE Robotics and Automation Letters*, *5*(4), 6001–6008.

Liu, C., Chen, W.-H., & Andrews, J. (2012). Tracking control of small-scale helicopters using explicit nonlinear MPC augmented with disturbance observers. *Control Engineering Practice*, *20*(3), 258–268.

Lofberg, J. (2004). YALMIP: A toolbox for modeling and optimization in MATLAB. In *IEEE international conference on robotics and automation* (pp. 284–289).

Maeder, U., Borrelli, F., & Morari, M. (2009). Linear offset-free model predictive control. *Automatica*, *45*(10), 2214–2222.

Mayne, D. Q. (2014). Model predictive control: Recent developments and future promise. *Automatica*, *50*(12), 2967–2986.

Mayne, D. Q., Rawlings, J. B., Rao, C. V., & Scokaert, P. O. (2000). Constrained model predictive control: Stability and optimality. *Automatica*, *36*(6), 789–814.

Mayne, D. Q., Seron, M. M., & Rakovic, S. (2005). Robust model predictive control of constrained linear systems with bounded disturbances. *Automatica*, *41*(2), 219–224.

Merckaert, K., Convens, B., El Makrini, I., Van der Perre, G., Nicotra, M. M., & Vanderborght, B. (2020). The explicit reference governor for real-time safe control of a robotic manipulator. In *IEEE/RSJ international conference on intelligent robots and systems*.

Ollero, A., Tognon, M., Suarez, A., Lee, D., & Franchi, A. (2021). Past, present, and future of aerial robotic manipulators. *IEEE Transactions on Robotics*, *38*(1), 626–645.

Pannocchia, G. (2015). Offset-free tracking MPC: A tutorial review and comparison of different formulations. In *European control conference* (pp. 527–532).

Pannocchia, G., & Bemporad, A. (2007). Combined design of disturbance model and observer for offset-free model predictive control. *IEEE Transactions on Automatic Control*, *52*(6), 1048–1053.

Pannocchia, G., Gabiccini, M., & Artoni, A. (2015). Offset-free MPC explained: Novelties, subtleties, and applications. *IFAC-PapersOnLine*, *48*(23), 342–351.

Pannocchia, G., & Rawlings, J. B. (2003). Disturbance models for offset-free model-predictive control. *AIChE Journal*, *49*(2), 426–437.

Rakovic, S. V., Kerrigan, E. C., Kouramas, K. I., & Mayne, D. Q. (2005). Invariant approximations of the minimal robust positively invariant set. *IEEE Transactions on Automatic Control*, *50*(3), 406–410.

Rashad, R., Bicego, D., Zult, J., Sanchez-Escalonilla, S., Jiao, R., Franchi, A., et al. (2022). Energy aware impedance control of a flying end-effector in the port-hamiltonian framework. *IEEE Transactions on Robotics*, *38*(6), 3936–3955.

Rawlings, J. B., Mayne, D. Q., & Diehl, M. (2017). *Model predictive control: Theory, computation, and design* (2nd ed.). Nob Hill Publishing Madison.

Rossiter, J. A. (2006). A global approach to feasibility in linear MPC. In *UK automatic control council international conference*.

Rossiter, J. A., & Kouvaritakis, B. (1998). Reference governors and predictive control. In *American control conference, Vol. 6* (pp. 3692–3693).

Ruggiero, F., Lippiello, V., & Ollero, A. (2018). Aerial manipulation: A literature review. *IEEE Robotics and Automation Letters*, *3*(3), 1957–1964.

Sariyildiz, E., Oboe, R., & Ohnishi, K. (2019). Disturbance observer-based robust control and its applications: 35th anniversary overview. *IEEE Transactions on Industrial Electronics*, *67*(3), 2042–2053.

Simon, D., Lofberg, J., & Glad, T. (2014). Reference tracking MPC using dynamic terminal set transformation. *IEEE Transactions on Automatic Control*, *59*(10), 2790–2795.

Tatjewski, P. (2014). Disturbance modeling and state estimation for offset-free predictive control with state-space process models. *International Journal of Applied Mathematics and Computer Science*, *24*(2).

Tognon, M., Alami, R., & Siciliano, B. (2021). Physical human-robot interaction with a tethered aerial vehicle: Application to a force-based human guiding problem. *IEEE Transactions on Robotics*, *37*(3), 723–734.

Wang, Y., & Xu, X. (2022). Disturbance observer-based robust control barrier functions. arXiv preprint arXiv:2203.12855.

Wang, H., Zuo, Z., Wang, Y., Yang, H., & Hu, C. (2022). Estimator-based turning control for unmanned ground vehicles: An anti-peak extended state observer approach. *IEEE Transactions on Vehicular Technology*, *71*(12), 12489–12498.

Xiao, W., Belta, C. A., & Cassandras, C. G. (2022). Sufficient conditions for feasibility of optimal control problems using control barrier functions. *Automatica*, *135*, Article 109960.

Xie, H., Dai, L., Lu, Y., & Xia, Y. (2021). Disturbance rejection MPC framework for input-affine nonlinear systems. *IEEE Transactions on Automatic Control*, *67*(12), 6595–6610.

Xu, X. (2018). Constrained control of input–output linearizable systems using control sharing barrier functions. *Automatica*, *87*, 195–201.

Yan, Y., Liu, C., Oh, H., & Chen, W.-H. (2021). Dual-layer optimization-based control allocation for a fixed-wing UAV. *Aerospace Science and Technology*, *119*, Article 107184.

Yunda Yan received the BEng degree in automation and the Ph.D. degree in control theory and control engineering from the School of Automation, Southeast University, Nanjing, China, in 2013 and 2019, respectively. From 2016 to 2018, he was a visting scholar with the Department of Biomedical Engineering, National University of Singapore, Singapore and the Department of Aeronautical and Automotive Engineering, Loughborough University, UK, respectively. From 2020 to 2022, he was a Research Associate with the Department of Aeronautical and Automotive Engineering, Loughborough University, UK. From 2022 to 2023, he was a Lecturer in Control Engineering with the School of Engineering and Sustainable Development, De Montfort University, UK. In Sep. 2023, he joined the Department of Computer Science, University College London, UK, as a Lecturer in Robotics and AI. His current research interest focuses on the safety-guaranteed control design for robotics, especially related to optimisation, data-driven and learning-based methods.

Xue-Fang Wang received the B.S. degree from the Ocean university of China, Qingdao college, in 2013. She obtained her Ph.D. degree in Control Theory and Control Engineering from Dalian University of Technology, Liaoning, China, in 2019. From 2017 to 2019, she was a visiting scholar to work with Prof. Andrew R. Teel at the University of California, Santa Barbara, US. From 2020 to 2023, she was a Research Associate at Dalian University of Technology, China, and Loughborough University, UK, respectively. She joined the School of Engineering, University of Leicester, UK, as a Lecturer in Control Engineering in 2023. Her main research interests are focused on multi-agent systems, hybrid systems, distributed optimisation problems, autonomous systems and model predictive control.

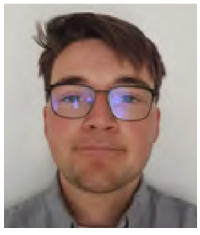

Benjamin James Marshall received the MEng degree from Loughborough University in Aeronautical Engineering (DIS). He is currently working towards a Ph.D. with the Loughborough Centre for Autonomous Systems. His research interests include quadcopter flight control and disturbance observer-based control.

Cunjia Liu received the Ph.D. degree in autonomous vehicle control from Loughborough University in 2011. He became an academic with Loughborough University in 2013 and is currently a Professor of Robotics and Autonomous Systems. His research cuts across the boundary between information fusion and control engineering with a focus on robotics and autonomous systems and their applications in defence, security, environment monitoring, and precision agriculture. He has published more than 100 peer reviewed papers and currently serves as an Associate Editor for IEEE Robotics and Automation and IEEE Robotics & Automation Magazine.

Jun Yang received the B.Sc. Degree in automation from the Department of Automatic Control, Northeastern University, Shenyang, China, in 2006, and a Ph.D. degree in control theory and control engineering from the School of Automation, Southeast University, Nanjing, China in 2011. He joined the Department of Aeronautical and Automotive Engineering at Loughborough University in 2020 as a Senior Lecturer and was promoted to a Reader in 2023. His research interests include disturbance observer, motion control, visual serving, nonlinear control and autonomous systems. He serves as Associate Editor or Technical Editor of IEEE Transactions on Industrial Electronics, IEEE-ASME Transactions on Mechatronics, IEEE Open Journal of Industrial Electronics Society, etc. He was the recipient of the EPSRC New Investigator Award. He is a Fellow of IEEE, IET and AAIA.

Wen-Hua Chen currently holds the Chair in Autonomous Vehicles with the Department of Aeronautical and Automotive Engineering, Loughborough University, Loughborough, U.K. He has a considerable experience in control, signal processing, and artificial intelligence, and their applications in robots, aerospace, and automotive systems. He has contributed significantly to a number of areas, including disturbance-observer-based control, model predictive control, and unmanned aerial vehicles. He is also a Chartered Engineer, a Fellow of IEEE, the Institution of Mechanical Engineers and the Institution of Engineering and Technology, U.K. He also holds a five years EPSRC Established Career Fellowship. He has authored or co-authored 300 papers and two books.